Probing BSM particles using inelastic nuclear scattering

Wei-Chih Huang
Texas A&M University
In collaboration with Bhaskar Dutta, Jayden Newstead, and Vishvas Pandey

Outline

1. Overview
2. Lab produced dark matter
3. Ambient dark matter (WIMP, boosted DM)
4. Axion
5. Conclusion

B. Dutta, W. Huang, J. L. Newstead 2302.10250; to appear
B. Dutta, W. Huang, J. L. Newstead and V. Pandey, PRD 106 (2022) 113006;
B. Dutta, W. Huang, D. Kim, J. Newstead, J. Pouk, to appear

Overview

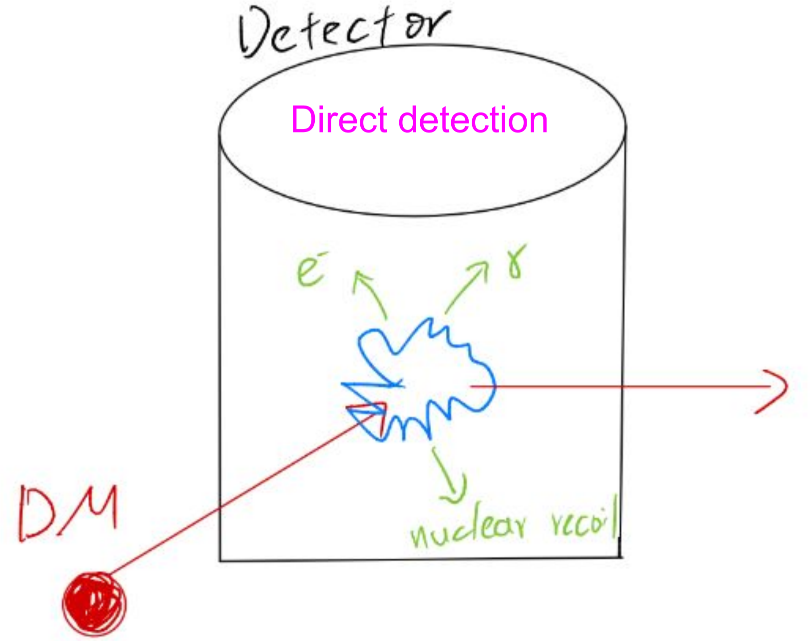

Any particle to search

$$\chi + N \rightarrow \chi + N^*$$

$$N^* \rightarrow N + \boxed{\gamma}$$

signal

For each of DM, WIMP, and axion

a. Theories and models
b. Benchmark experiments
c. Results

Light dark matter in stopped pion experiment

Pros

- Lower background
- Little to none threshold effect

Cons

- Lower signal
- More calculations

Inelastic DM-Nucleus Scattering

$$\mathcal{L} \supset g_D A'_\mu \bar{\chi}\gamma^\mu \chi + e\epsilon Q_q A'_\mu \bar{q}\gamma^\mu q$$

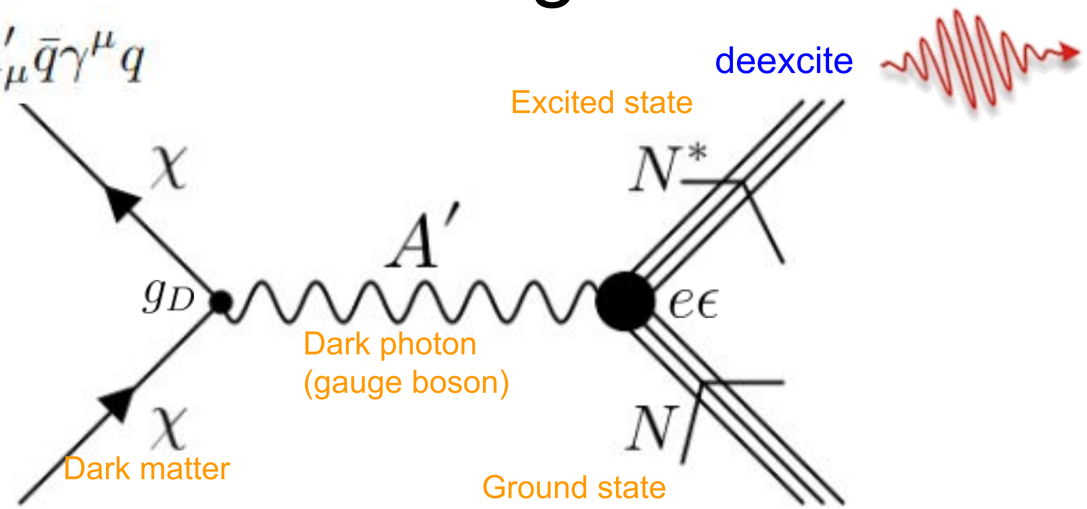

Q: Why not elastic?

A: Elastic has high signal rates but also high background (keV nuclear recoil)

$$\frac{d\sigma^{DM}_{\rm el}}{dE_r} = \frac{e^2\epsilon^2 g_D^2 Z^2}{4\pi(E_\chi^2 - m_\chi^2)(2m_N E_r + m_{A'}^2)^2} F^2(E_r) \times \left[2E_\chi^2 m_N\left(1 - \frac{E_r}{E_\chi} - \frac{m_N E_r}{2E_\chi^2}\right) + E_r^2 m_N\right]$$

Multipole expansion

J. D. Walecka, 2004;
W. Haxton, et al., 0706.2210

In Standard Model…

$$\langle f|\hat{H}_W|i\rangle = \frac{G_F}{\sqrt{2}}\int d^3x \langle f|j_\mu^{lep}\hat{\mathcal{J}}^\mu(\vec{x})|i\rangle$$

$$= \frac{G_F}{\sqrt{2}}\int d^3x\, e^{-i\vec{q}\cdot\vec{x}}\left(l_0\mathcal{J}^0(\vec{x}) - \vec{l}\cdot\boldsymbol{\mathcal{J}}(\vec{x})\right)$$

Spherical decompsition

Multipole operator $\hat{\mathcal{M}}_{JM}(q) \equiv \int d^3x\,[j_J(qx)Y_{JM}(\Omega_x)]\,\hat{\mathcal{J}}^0(\vec{x})$

Nuclear response function $M_{JM}(q\vec{x}_i) \equiv j_J(qx_i)Y_{JM}(\Omega_{x_i})$

where Y_{JM} is Bessel spherical harmonics

$$l_\mu = \bar{\chi}\gamma^\mu\chi.$$

$$\frac{d\sigma_{\rm inel}^{DM}}{dE_r} = \frac{2e^2\epsilon^2 g_D^2 {E'}_\chi^2}{p_\chi {p'}_\chi (2m_N E_r + m_{A'}^2)^2}\frac{m_N}{2\pi}\frac{4\pi}{2J+1}\left\{\sum_{J\geqslant 1,spin}\left[\frac{1}{2}(\vec{l}\cdot\vec{l}^* - l_3 l_3^*)\left(|\langle J_f||\hat{\mathcal{T}}_J^{mag}||J_i\rangle|^2 + |\langle J_f||\hat{\mathcal{T}}_J^{el}||J_i\rangle|^2\right)\right]\right.$$

$$\left. + \sum_{J\geqslant 0,spin}\left[l_0 l_0^*\,|\langle J_f||\hat{\mathcal{M}}_J||J_i\rangle|^2 + l_3 l_3^*\,|\langle J_f||\hat{\mathcal{L}}_J||J_i\rangle|^2 - 2\,l_3 l_0^* Re\left(\langle J_f||\hat{\mathcal{L}}_J||J_i\rangle\langle J_f||\hat{\mathcal{M}}_J||J_i\rangle^*\right)\right]\right\}$$

Nuclear Shell Model Code: BIGSTICK

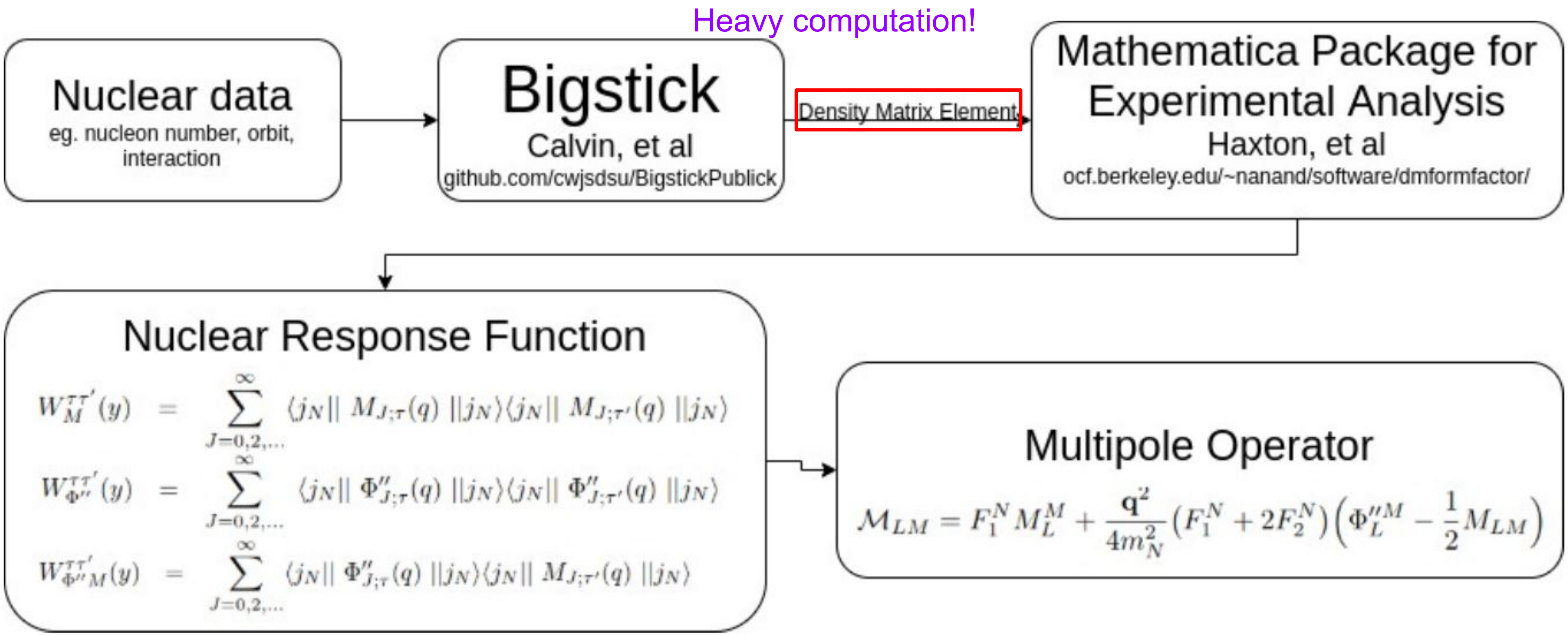

It takes a long time and needs tons of RAM and CPU

Is there a shortcut?

Long Wavelength Limit

$$\hat{\mathcal{M}}_{JM}(q) = \frac{q^J}{(2J+1)!!}\int d^3x x^J Y_{JM}\hat{\mathcal{J}}_0(\mathbf{x})$$

$$\hat{\mathcal{L}}_{JM}(q) = \frac{-iq^{J-1}}{(2J+1)!!}\int d^3x x^J Y_{JM}\nabla\cdot\hat{\mathcal{J}}(\mathbf{x})$$

$$\hat{\mathcal{T}}^{el}_{JM}(q) = -i\frac{q^{J-1}}{(2J+1)!!}\left(\frac{J+1}{J}\right)^{1/2}\int d^3x x^J Y_{JM}\nabla\cdot\hat{\mathcal{J}}(\mathbf{x})$$

$$\hat{\mathcal{T}}^{mag}_{JM}(q) = i\frac{q^J}{(2J+1)!!}\left(\frac{J+1}{J}\right)^{1/2}\int d^3x\left[\frac{1}{J+1}\mathbf{r}\times\hat{\mathcal{J}}(\mathbf{x})\right]\cdot\nabla x^J Y_{JM}$$

The surviving multipoles are $\hat{\mathcal{M}}_{00}, \hat{\mathcal{L}}_{1M}, \hat{\mathcal{T}}^{el}_{1M}$.

$$\hat{\mathcal{M}}_{00} = \frac{1}{\sqrt{4\pi}}F_1\sum_{i=1}^{A}\hat{FT}\,(\sim\hat{\tau})$$

Fermi doesn't contribute to inelastic scattering because it's even-even operator. It only exists in elastic scattering

$$\hat{\mathcal{T}}^{el}_{1M} = \sqrt{2}\hat{\mathcal{L}}_{1M} = \frac{i}{\sqrt{6\pi}}G_A\sum_{i=1}^{A}\hat{GT}\,(\sim\hat{\sigma}\hat{\tau})$$

Is GT (Gamow Teller) the shortcut?

Strength and Multipole in BIGSTICK

BIGSTICK can calculate the strength of a given operator

$$\left|(\Psi_f : J_f||\hat{O}_J||\Psi_i J_i)\right|^2$$

	Strength	Multipole
Time	Short	Long
RAM & CPU	Light	Heavy
Output	Less detailed The strength and energy	Comprehensive Density matrix -> strength

Multipole has energy, spin, isospin, and density matrix
Strength only has energy, strength

GT Strength Lines

eg. Ar40

$$\Delta J = |J_f - J_i| = 1$$

GT strength = $|\langle J_f || \sum_{i=1}^{A} \frac{1}{2} \hat{\sigma}_i \hat{\tau}_0 || J_i \rangle|^2$

excited state (J_f) ground state (J_i)

one line = one transition = one excited state

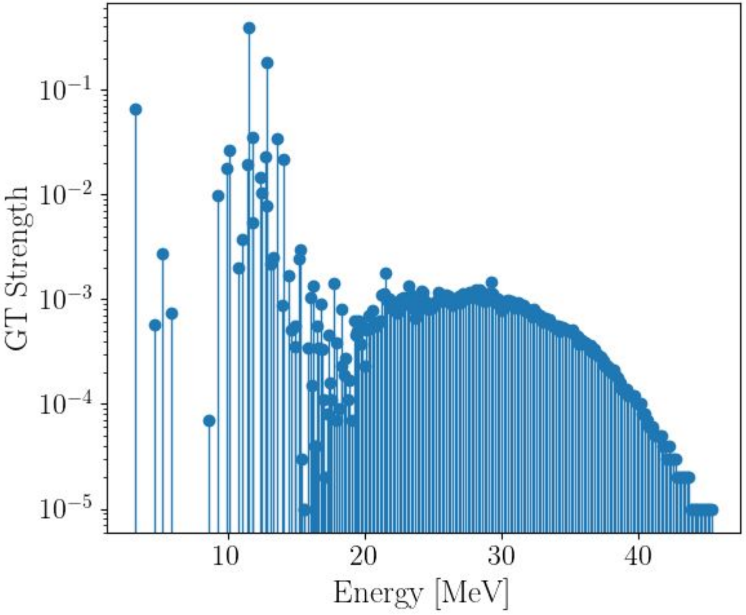

convoluted with 150 keV width Gaussian

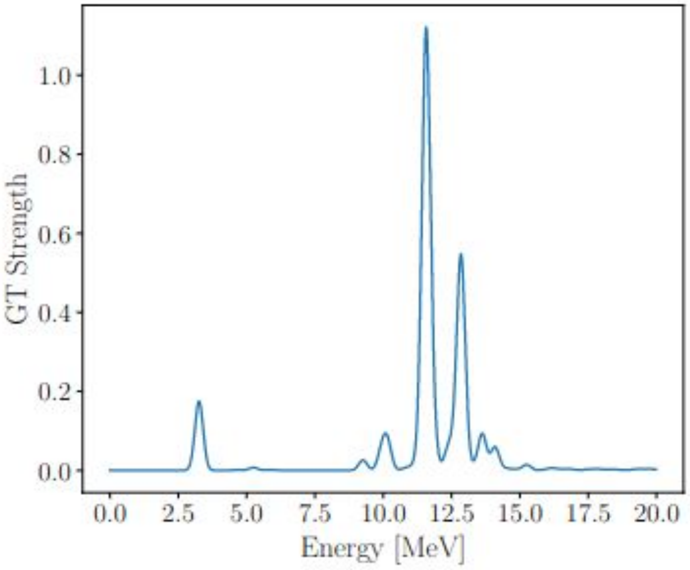

Experiment data

E^* [keV]	J^π
0.0^a	0^+
$1460.851(6)^a$	2^+
$2120.8(3)^b$	0^+
$2524.1(2)^b$	2^+
$2892.6(1)^a$	4^+
3208.0(6)	2^+
$3464.5(1)^a$	6^+
3511.3(5)	2^+
$3515(1)^b$	4^+
3680.8(2)	3^-
3918.8(2)	2^+
3941.7(3)*	
4041(1)	N
4082.5(2)	3^-
4178.9(3)*	
4226(1)	4^-
4229(1)	$1^+,2^-,3^+$
4300.8(3)	$\langle 1,3\rangle^-$
4324.5(3)	2^+
4358.0(3)	N
4420(1)	$\langle 0^+–4^+\rangle$
4427(1)	$\langle 4^+\rangle$
4473(1)	1
4481.0(3)	1^-
$4494(1)^c$	5^-
4562.3(2)	$\langle 1,3\rangle^-$
4578(1)	$\langle 2^+,3^-\rangle$
4602(1)	$\langle 0^+–4^+\rangle$
4674(1)	$1^+,2^-,3^+$
4737.8(4)*	
4769.0(3)	1^-

Cross Section in Long Wavelength Limit

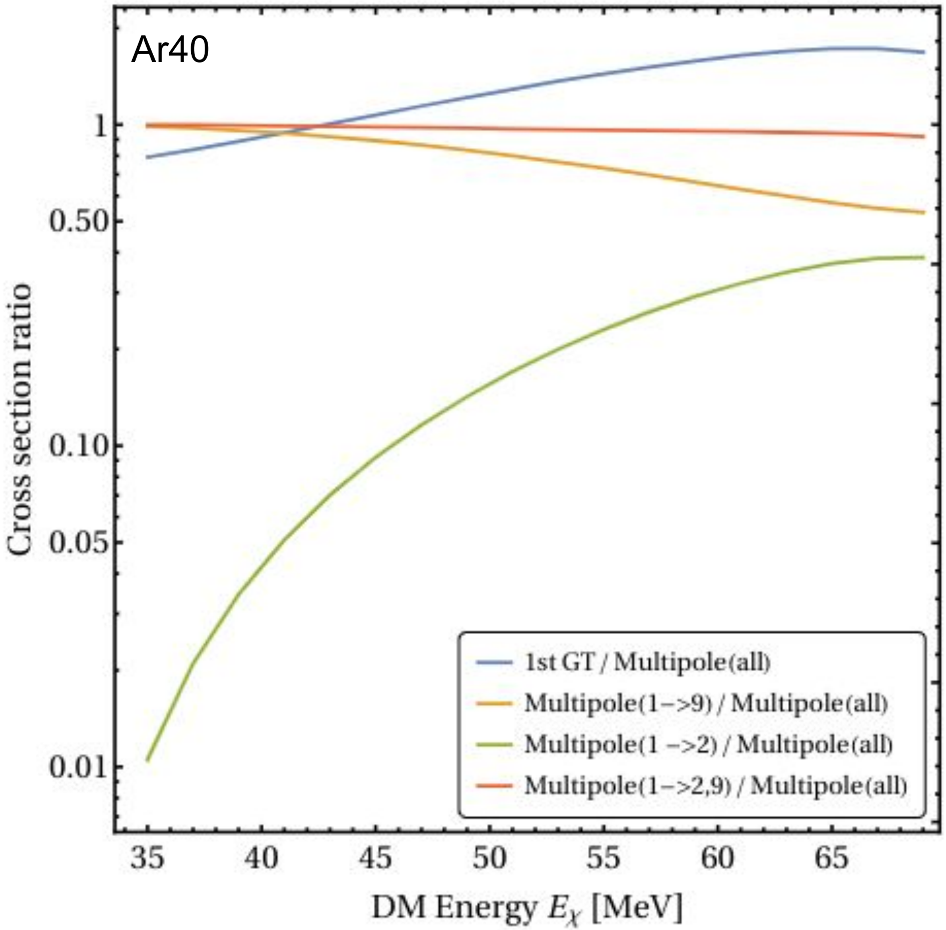

$$E_r \to 0$$

$$\frac{d\sigma^{DM}_{inel}}{d\cos\theta} = \frac{2e^2\epsilon^2 g_D^2 E'^2_\chi}{(2m_N E_r + m^2_{A'})^2}\frac{1}{2\pi}\frac{4\pi}{2J+1} \times \sum_{s_i,s_f} \vec{l}\cdot\vec{l}^* \frac{g_A^2}{12\pi}\left|\langle J_f\right|\left|\sum_{i=1}^{A}\frac{1}{2}\hat{\sigma}_i\hat{\tau}_0\right|\left|J_i\rangle\right|^2$$

Gamow-Teller (GT) operator

GT strength is the shortcut

Er in keV, DM in MeV or above
=> GT is a good approximation

B. Dutta, W. Huang, J. L. Newstead and V. Pandey, PRD 106 (2022) 113006

DM-Nucleus Scattering: Elastic vs Inelastic

$$\frac{d\sigma_{\rm el}^{DM}}{dE_r} = \frac{e^2\epsilon^2 g_D^2 Z^2}{4\pi(E_\chi^2-m_\chi^2)(2m_N E_r+m_{A'}^2)^2}F^2(E_r) \times \left[2E_\chi^2 m_N\left(1-\frac{E_r}{E_\chi}-\frac{m_N E_r}{2E_\chi^2}\right)+E_r^2 m_N\right]$$

$$\frac{d\sigma_{inel}^{DM}}{d\cos\theta} = \frac{2e^2\epsilon^2 g_D^2 E'^2_\chi}{(2m_N E_r+m_{A'}^2)^2}\frac{1}{2\pi}\frac{4\pi}{2J+1} \times \sum_{s_i,s_f}\vec{l}\cdot\vec{l}^*\frac{g_A^2}{12\pi}|\langle J_f||\sum_{i=1}^{A}\frac{1}{2}\hat{\sigma_i}\hat{\tau_0}||J_i\rangle|^2$$

For Ar40

$$\left(\frac{Inelastic}{Elastic}\right)_{signal} = 10^{-2}-10^{-1}$$

$$\left(\frac{Inelastic}{Elastic}\right)_{bkg} = 10^{-4}-10^{-3}$$

Inelastic search can be better

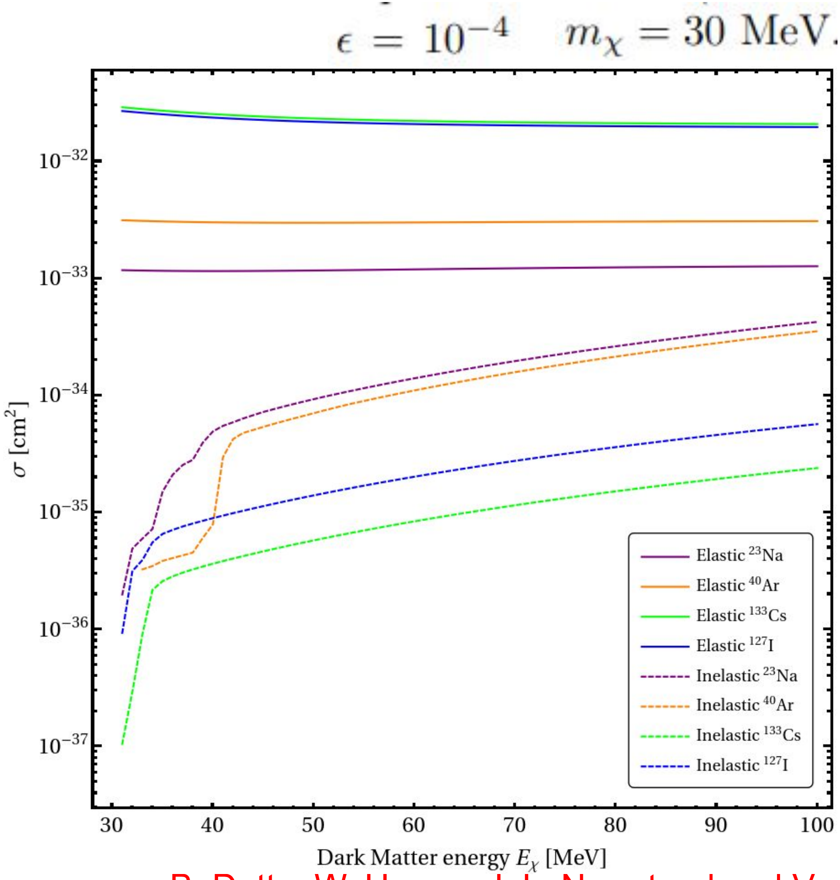

B. Dutta, W. Huang, J. L. Newstead and V. Pandey, PRD 106 (2022) 113006

Inelastic DM-Nucleus Scattering

Cross section has the same form for fermion and scalar DM, only difference is the current $l_\mu = \bar{\chi}\gamma^\mu\chi$.

$$\frac{d\sigma_{inel}^{DM}}{d\cos\theta} = \frac{2e^2\epsilon^2 g_D^2 E'^2_\chi}{(2m_N E_r + m_{A'}^2)^2}\frac{1}{2\pi}\frac{4\pi}{2J+1} \times \sum_{s_i,s_f}\vec{l}\cdot\vec{l}^*\frac{g_A^2}{12\pi}|\langle J_f||\sum_{i=1}^{A}\frac{1}{2}\hat{\sigma}_i\hat{\tau}_0||J_i\rangle|^2$$

Fermion $\quad \mathcal{L}_f \supset g_D A'_\mu\bar{\chi}\gamma^\mu\chi + e\epsilon Q_q A'_\mu\bar{q}\gamma^\mu q$

$$\sum_{s_i,s_f}\vec{l}\cdot\vec{l}^* = 3 - \frac{1}{E_\chi E'_\chi}\left[\frac{1}{2}\left(p_\chi^2 + p'^2_\chi - 2m_N E_r\right) + \frac{3m_\chi^2}{4}\right]$$

Scalar $\quad \mathcal{L}_s \supset |D_\mu\phi|^2 + e\epsilon Q_q A'_\mu\bar{q}\gamma^\mu q$

$$\vec{l}\cdot\vec{l}^* = \frac{1}{2E_\chi E'_\chi}\left(p_\chi^2 + p'^2_\chi - 2m_N E_r\right)$$

Experiments and Detectors

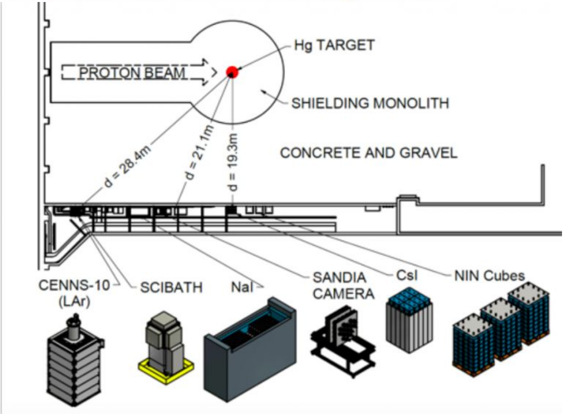

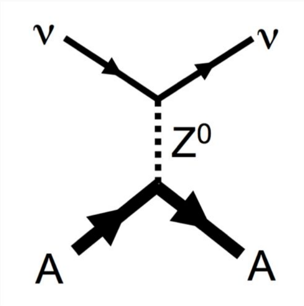

+

+

CAPTAIN = "Cryogenic Apparatus for Precision Tests of Argon Interactions with Neutrinos"

Why NaI and CCM?
They have large detector mass

Experiment	E_{beam} [GeV]	POT [yr^{-1}]	Target	Detector: target	mass	distance	angle	E_r^{th}
COHERENT	1	1.5×10^{23}	Hg	CsI[Na]	14.6 kg	19.3 m	90°	6.5 keV
				NaI[Tl]	185 kg	22 m	120°	900 keV
				NaI[Tl]	3500 kg	22 m	120°	~few keV
CCM	0.8	1.0×10^{22}	W	Ar	7 t	20 m	90°	25 keV

DM Flux in CCM

$A' \to \chi\bar{\chi}$ Decay in < O(-10) ns

$$\pi^- + p \to n + A'$$
$$\pi^0 \to \gamma + A'$$ dominant
$$\eta^0 \to \gamma + A'$$
$$e^{\pm *} \to e^{\pm} + A'$$

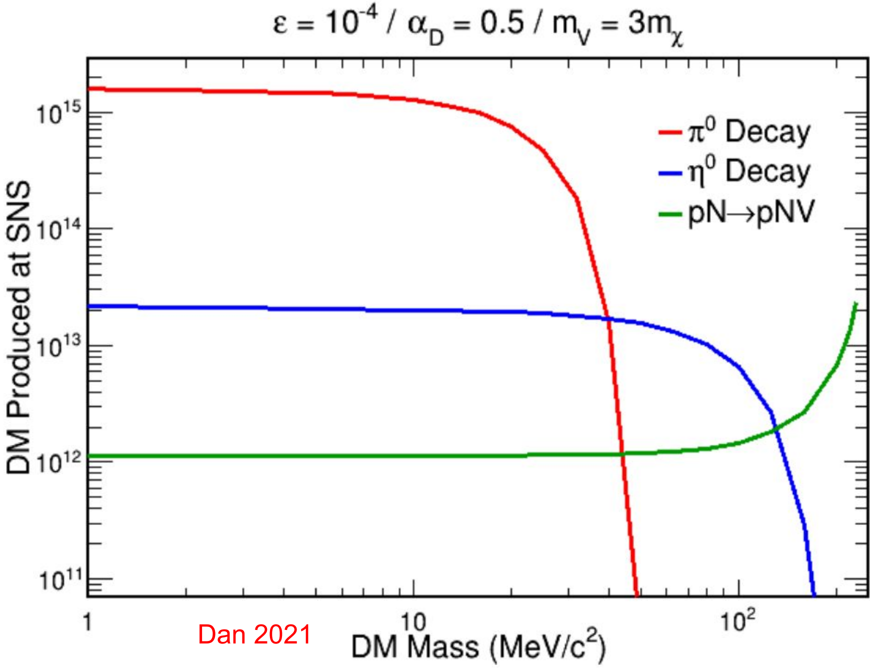

Dan 2021

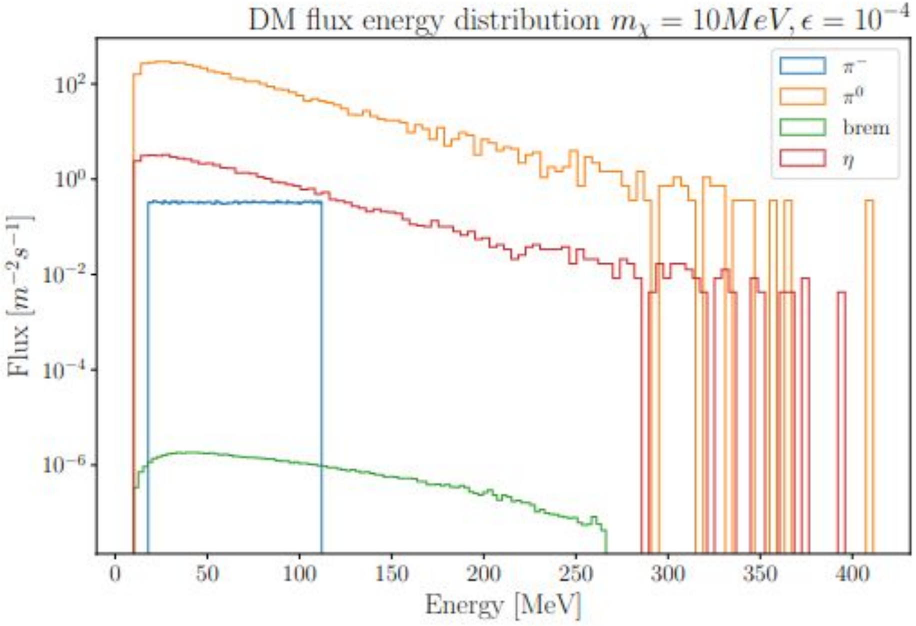

Prompt Window

Signal = inelastic DM from pion and eta decay
Bkg = inelastic prompt neutrino → Remove ν_e → No bkg due to charge current

$$\tau_\eta \sim 10^{-10} ns$$

$$\tau_{\pi^0} \sim 10^{-7} ns$$

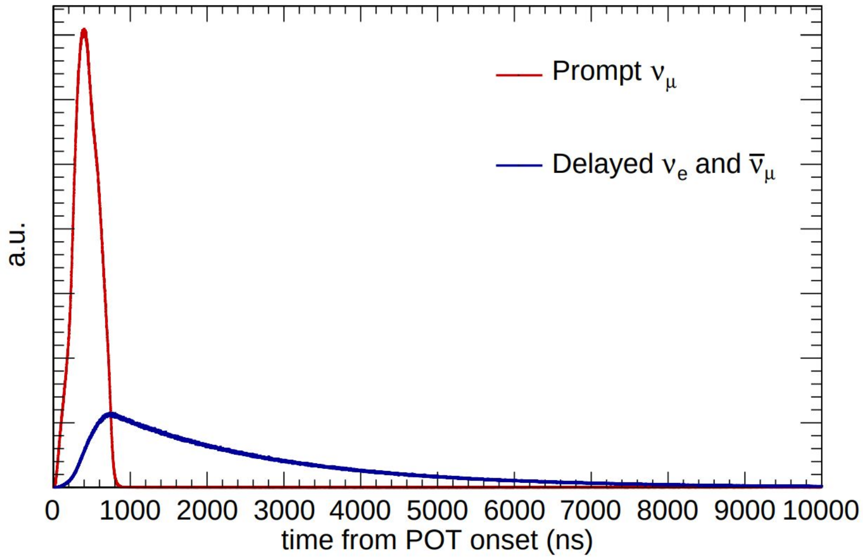

Inelastic nu background

Detector	CCM (LAr)	COHERENT (NaI)
Delayed + prompt	327	462
Prompt only (t<1ms)	64.8	106
220ns cut (to 5%)	3.24	5.3

220ns = 150ns (beam arrival) + 70ns (relativistic travel for 20 meter)

CCM 2112.09979;
Phys. Rev. D, 106(1):012001, 2022

Background

Detector	Bkg estimation*
COHERENT NaI	~O(100)
CCM	~O(100)

*1/100 Background reduction applied

NaI (COHERENT) is ongoing, we assumed similar background as CCM

CCM Collaboration, A. A. Aguilar-Arevalo et al., 2022

Rescale the GT strength (0.162) to be consistent with the experiment

W. Tornow et al., 2210.14316

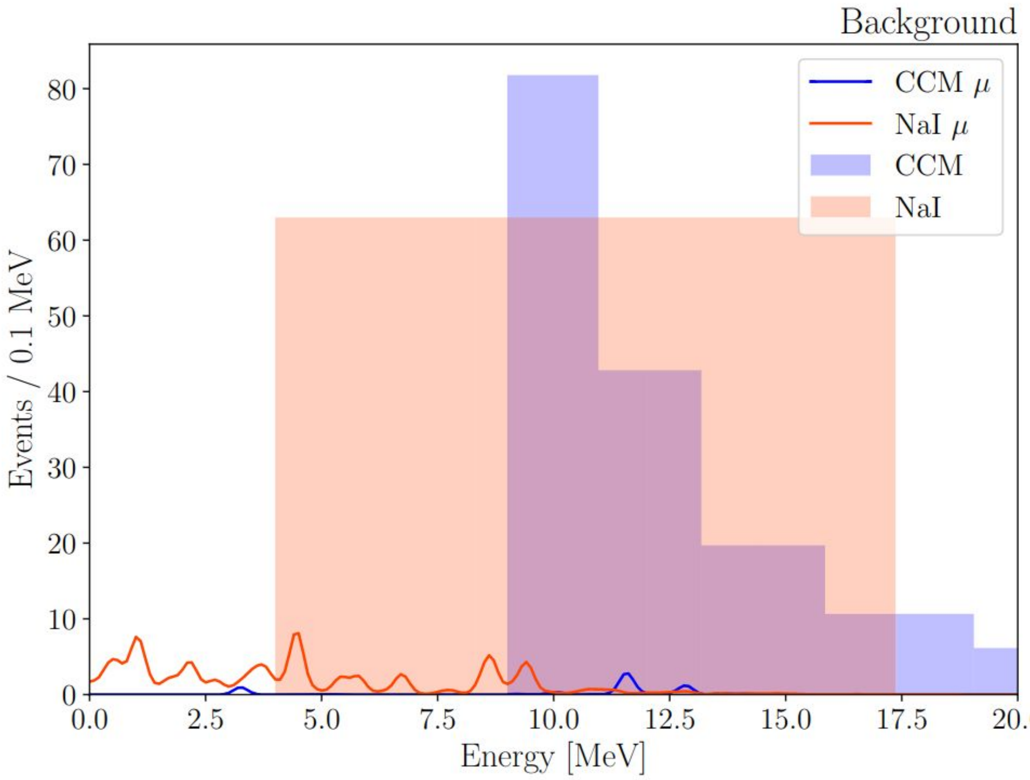

Baishan's calculation on many (~30) multipole states shows that GT indeed works

Baishan Hu, to be appear

Background

Detector	Bkg estimation
PIP2BD	~700

~GeV beam
100t LAr
4.95e23 POT total
Proposed beam dump experiment at Fermilab
Bkg is scaled from CCM by relative POT ratio

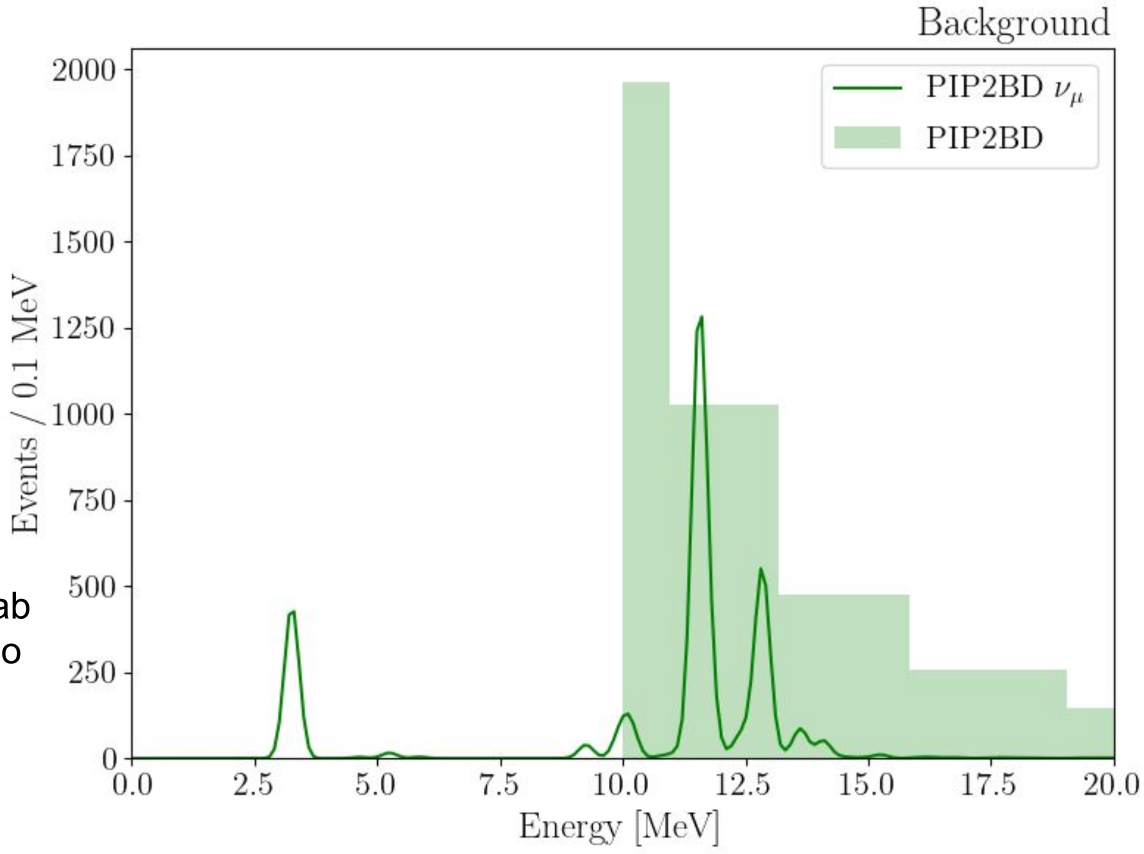

M. Toups et al., 2203.08079

Sensitivities Plot

$$\sigma_{\text{elastic}} \sim 1/(2m_N E_r + m_{A'}^2)^2$$
$$\approx 1/(2m_N E_r)^2 \text{ if } m_{A'}^2 < 2m_N E_r$$

Dashed is our calculation

$g_D = \sqrt{2\pi}$

$m_{A'}/m_\chi = 3$

Er~O(10) keV causes the flatness in the sensitivity curve for elastic nuclear scattering

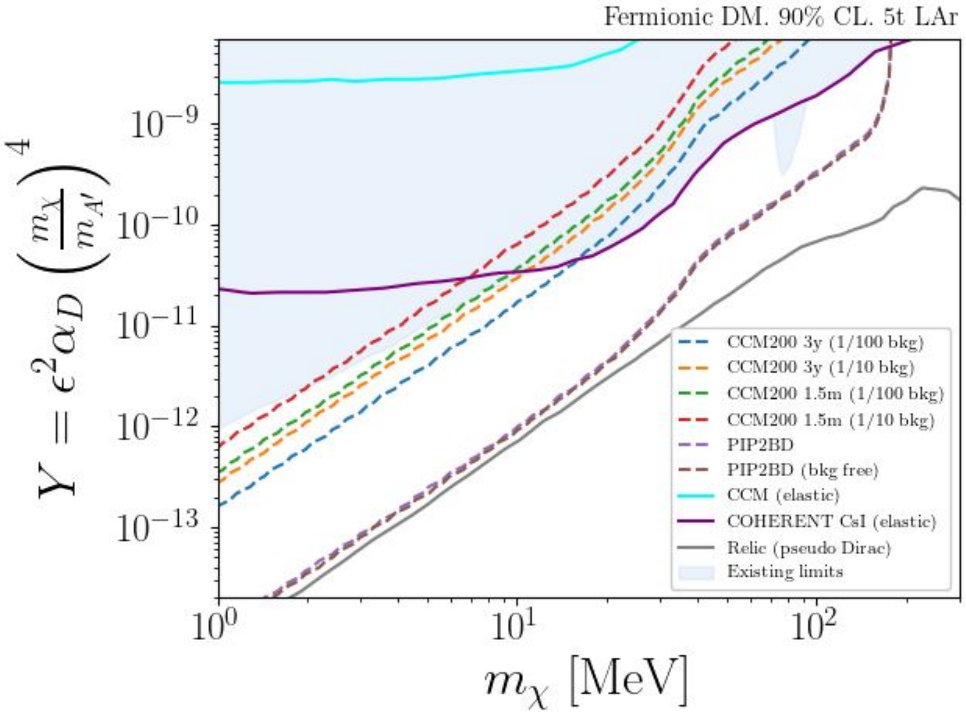

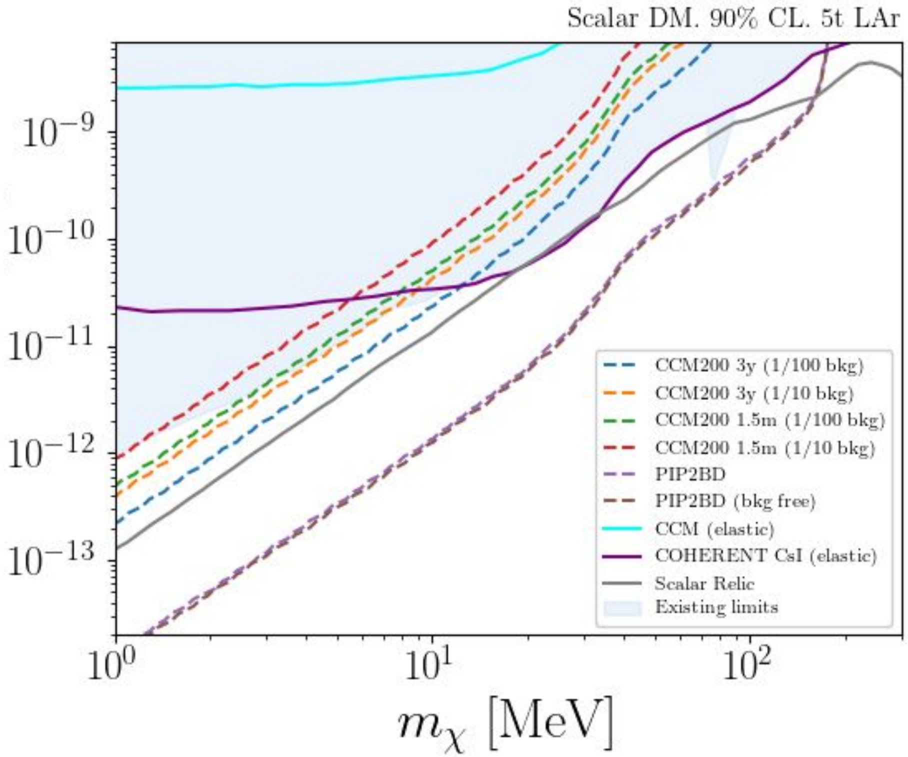

Sensitivities Plot

COHERENT Collaboration, 2205.12414;
A. A. Aguilar-Arevalo et al, 2109.14146

Dashed is our calculation

$$m_{A'}/m_\chi \approx 2$$

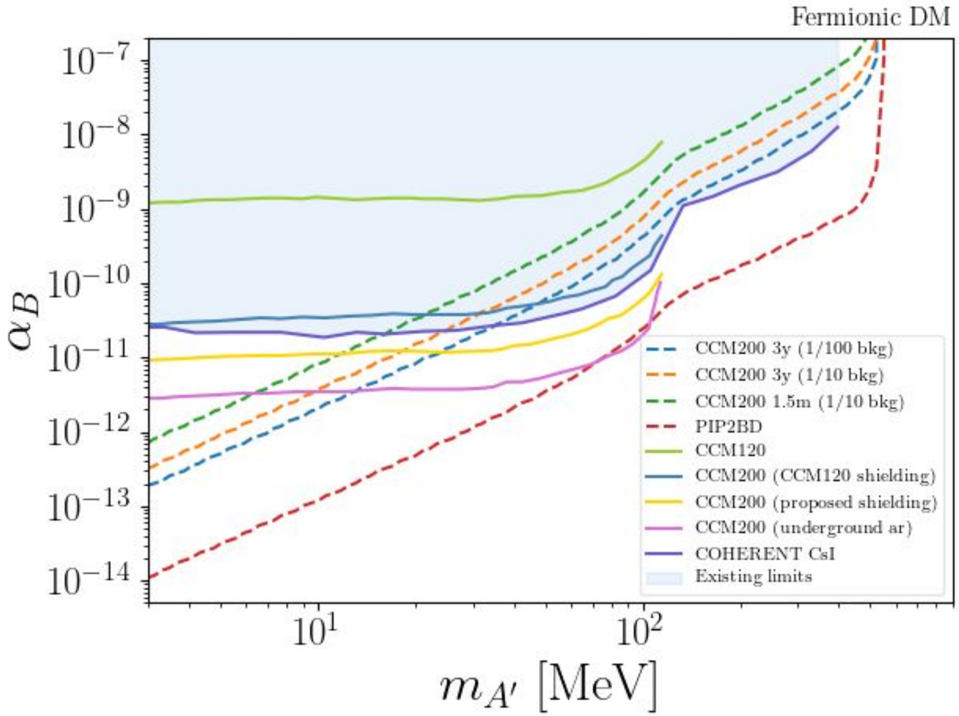

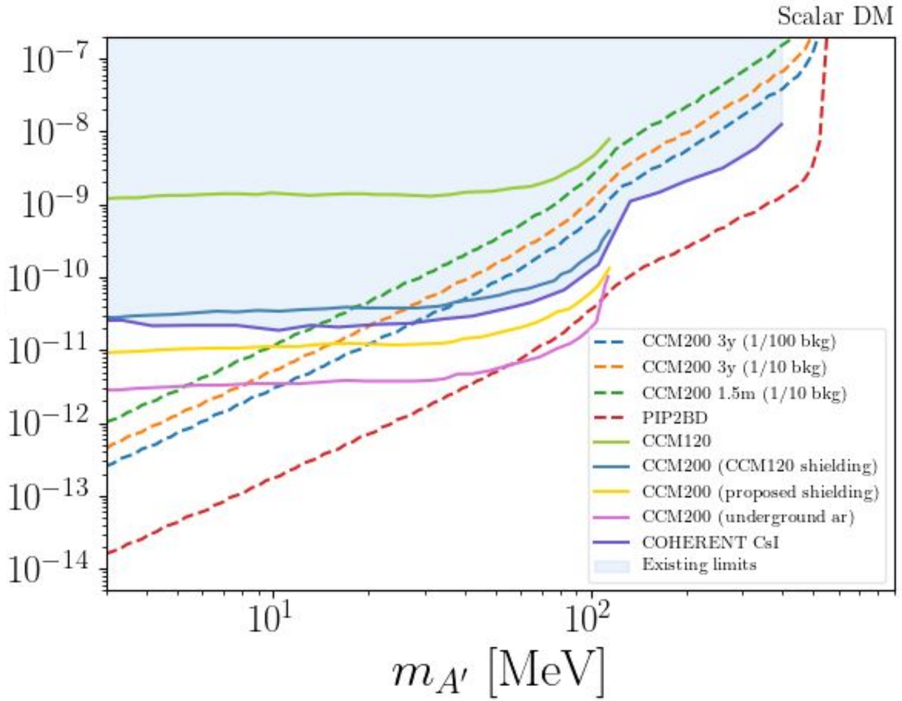

WIMP & Ambient DM

Interaction and cross section

$$\mathcal{L} \supset g_D A'_\mu \bar{\chi}\gamma^\mu \chi + e\epsilon Q_q A'_\mu \bar{q}\gamma^\mu q$$

Same as light DM

$$\frac{d\sigma^{DM}_{inel}}{d\cos\theta} = \frac{2e^2\epsilon^2 g_D^2 E'_\chi p'_\chi}{(2m_N E_r + m_{A'}^2)^2} \frac{1}{2\pi} \frac{4\pi}{2J+1}$$
$$\times \boxed{r_\chi} \sum_{s_i, s_f} \vec{l} \cdot \vec{l}^* \frac{g_A^2}{12\pi} |\langle J_f || \sum_{i=1}^{A} \frac{1}{2} \hat{\sigma}_i \hat{\tau}_0 || J_i \rangle|^2$$

A correction factor due to large mass of DM

$$r_\chi = \left[1 + \frac{E_\chi}{m_N}(1 - \cos\theta)\right]^{-1}$$

$$r_\chi \to 1 \text{ if } m_N \gg m_\chi$$

Experiments

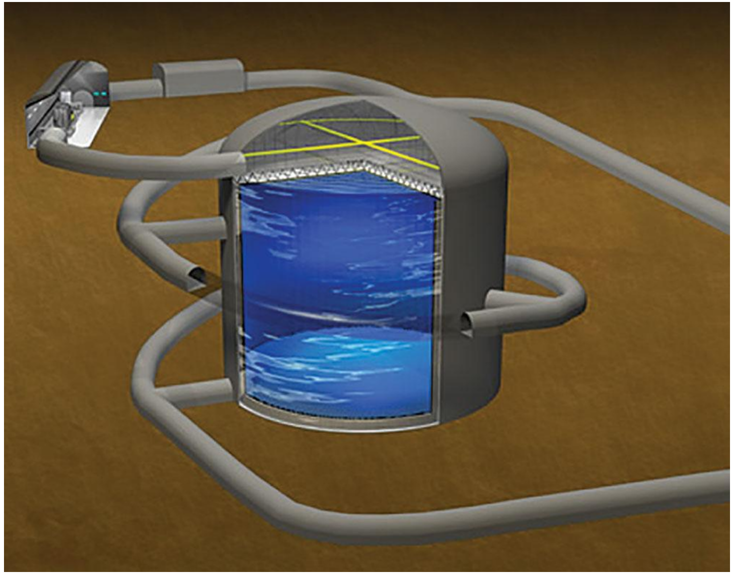

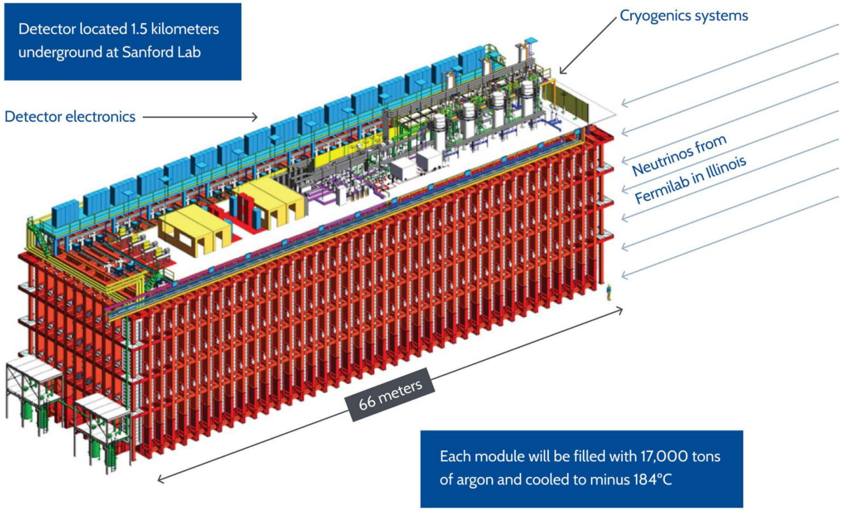

Experiment	Material	Geometry
HyperK	188kton water	78m tall, 74m diameter
DUNE	40kton Ar40	L: 65.8m, W: 18.9m, H: 17.8m

BIGSTICK GT strength

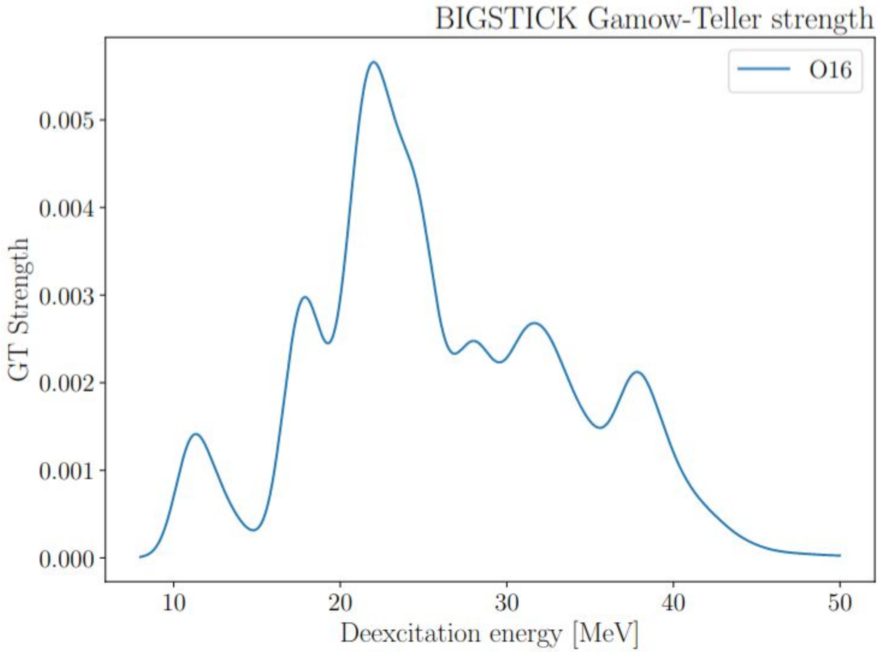

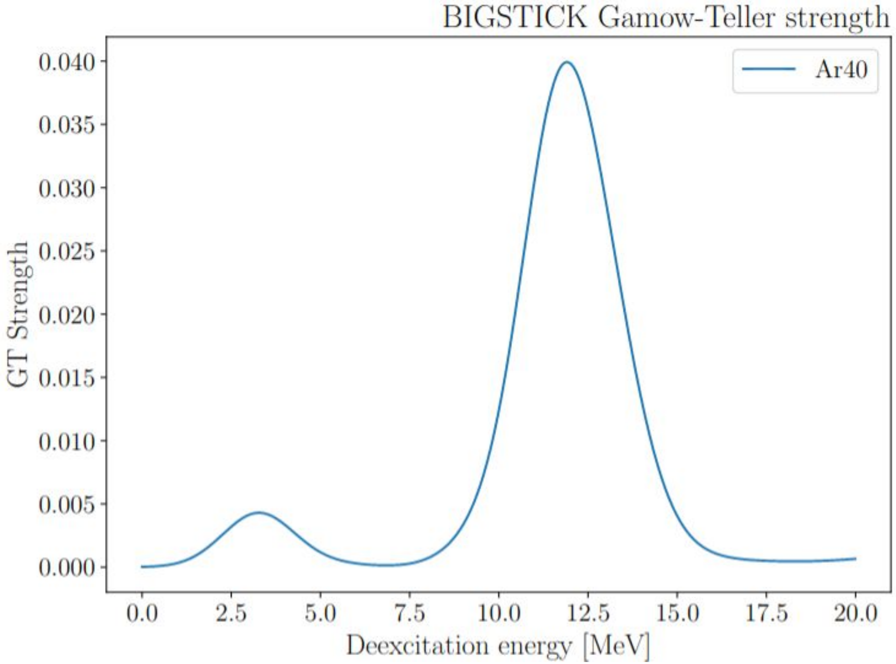

Backgrounds

M. Honda et al., PRD 92, 023004, 2015;
Yoichiro Suzuki, 2000

$$\nu + N \to \nu + N^*$$
$$N^* \to N + \gamma$$

Inelastic neutrino scattering

$$\sigma_\nu^{\mathrm{GT}} \approx \frac{G_f^2 g_A^2}{\pi(2J+1)} (E_\nu - \Delta E)^2 \left| \left\langle J_f \left\| \sum_{i=1}^{A} \frac{1}{2} \hat{\sigma}_i \hat{\tau}_0 \right\| J_i \right\rangle \right|^2$$

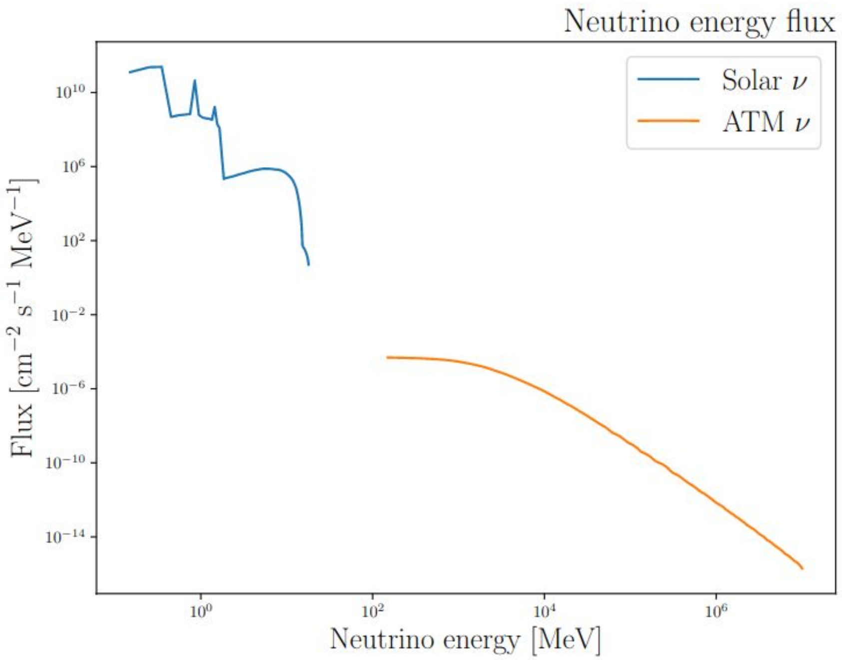

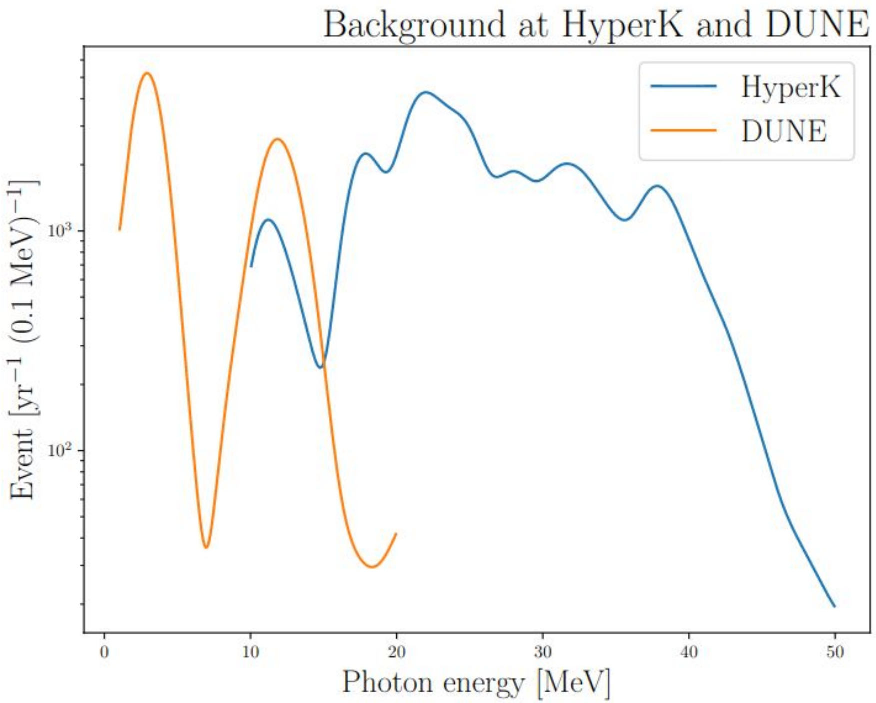

Sensitivities Plot

Ambient WIMP
Boosted DM

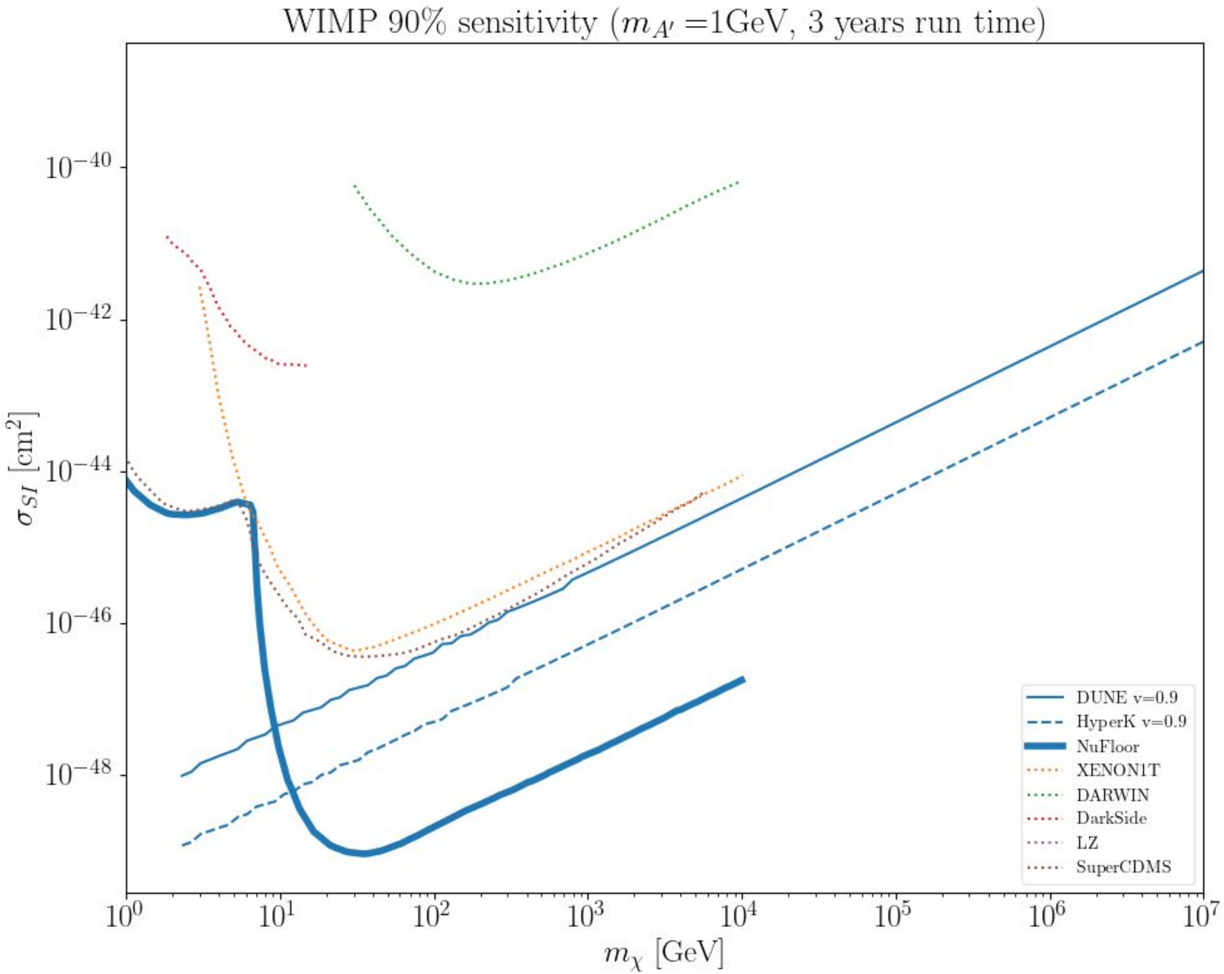

Axion

Interaction

$$\mathcal{L}_{\text{int}} \supset \frac{\partial_\mu a}{f_a} \bar{N} \gamma^\mu \gamma^5 N - \frac{1}{4} g_{a\gamma\gamma} a F_{\mu\nu} \tilde{F}^{\mu\nu}$$

$$g_{ann} = \frac{1}{f_a}$$

a is axion (pseudoscalar)

g_{ann} and $g_{a\gamma\gamma}$ have dimension E^{-1}

Δ_1 = deexcitation energy $\ll m_N$ (source/production)

Δ_2 = excitation energy $\ll m_N$ (absorption/detection)

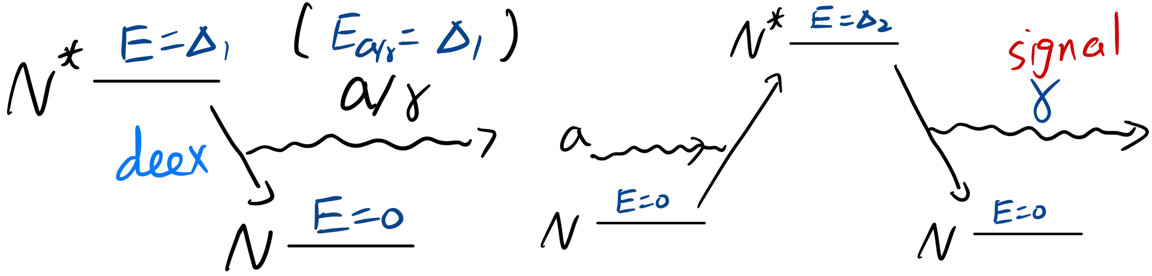

Production	**Coupling**
Nuclear deexcitation $N^* \to N + \gamma/a$	g_{ann}
Primakoff $\gamma + e^-/N \to a + e^-/N$	$g_{a\gamma\gamma}$
Detection	
Nuclear absorption $a + N \to N^* \to N + \gamma$	g_{ann}
Inverse Primakoff $a + N \to \gamma + N$	$g_{a\gamma\gamma}$
Decay $a \to 2\gamma$	$g_{a\gamma\gamma}$

Production cross sections

B. Dutta, W. Huang, J. Newstead

Primakoff $$\frac{d\sigma_P^p}{d\cos\theta} = \frac{1}{4} g_{a\gamma\gamma}^2 \alpha Z^2 F^2(t) \frac{|\vec{p}_a|^4 \sin^2\theta}{t^2}$$ $$t = m_a^2 + E_\gamma (E_a - p_a \cos\theta)$$

Nuclear lines at target

Channel	E_γ (keV)	Transitions	Φ_γ (fission^{-1})	(GCi)
p(n,γ)d	2230	Isovector M1	0.25	0.61
^{10}B(n,α)^{7}Li*	478	M1 $(\frac{1}{2}^-) \to (\frac{3}{2}^-)$	0.28	0.68
^{91}Y*	555	M4 $(\frac{9}{2}^+) \to (\frac{1}{2}^-)$	0.024	0.058
^{97}Nb*	743	M4 $(\frac{1}{2}^-) \to (\frac{9}{2}^+)$	0.055	0.13
^{135}Xe*	526	M4 $(\frac{11}{2}^-) \to (\frac{3}{2}^+)$	0.0097	0.023
^{137}Ba*	662	M4 $(\frac{11}{2}^-) \to (\frac{3}{2}^+)$	0.0042	0.010

Detection cross sections

$$\Gamma(a \to 2\gamma) = \frac{g_{a\gamma\gamma}^2 m_a^3}{64\pi}$$

$$\frac{d\sigma_{\text{invPri}}}{d\cos\theta} = \frac{1}{2} g_{a\gamma}^2\, \alpha\, Z^2 F^2(t) \frac{p_a^4\, sin^2\theta}{t^2}$$

$$\sigma_{\text{abs}} = g_{ann}^2 2\pi \delta(E_a - E_r - \Delta_2) p_a \cdot F$$

Gamow Teller cross section

$$\sigma_{\text{abs}}(E_a, \Delta_2) = \frac{g_A^2 \pi}{6(2J+1)} g_{ann}^2 \delta(E_a - E_r - \Delta_2)\, p_a\, |\langle J_f || \sum_{i=1}^{A} \frac{1}{2} \hat{\sigma}_i \hat{\tau}_0 || J_i \rangle|^2$$

M and E transitions

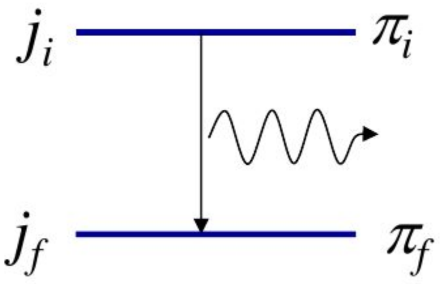

$$|J_i - J_f| \le J \le J_i + J_f$$
$$\pi = \pi_i \pi_f$$

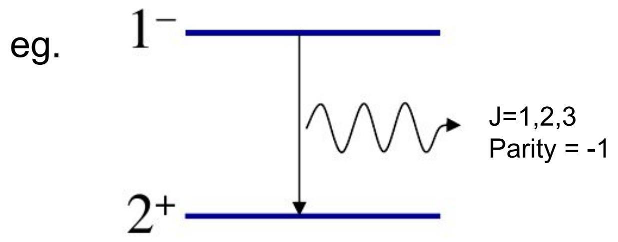

$$J^\pi = 1^-(E1), 2^-(M2), 3^-(E3)$$

Axion is pseudo scalar => -1 parity => M trans

$$\pi = (-1)^I \text{ for E transitions}$$
$$\pi = (-1)^{I+1} \text{ for M transitions}$$
$$\text{multipolarity} = 2^I$$

I	π_γ	Radiation type	Label
1	–1	Electric Dipole radiation	E1
1	+1	Magnetic Dipole radiation	M1
2	–1	Magnetic Quadrupole radiation	M2
2	+1	Electric Quadrupole radiation	E2
3	–1	Electric Octapole radiation	E3
3	+1	Magnetic Octapole radiation	M3

Nuclear deexcitation lines

$N^* \rightarrow N + \gamma$ Photon energy E_γ, Flux Φ_γ

Nucleon coupling model g_{ann}

$N^* \rightarrow N + a$ Axion energy E_a, Flux Φ_a

This table uses 2.9GW power reactor, but we use 1MW, so scaling is required

$1\text{Ci} = 3.7 \times 10^{10}$ decay per second

$1\text{GCi} = 10^{9}\text{Ci}$

Channel	E_γ (keV)	Transitions	Φ_γ (fission^{-1})	(GCi)
p(n,γ)d	2230	Isovector M1	0.25	0.61
^{10}B(n,α)^{7}Li*	478	M1 $(\frac{1}{2}^-) \rightarrow (\frac{3}{2}^-)$	0.28	0.68
~~^{91}Y*~~	~~555~~	~~M4 $(\frac{9}{2}^+) \rightarrow (\frac{1}{2}^-)$~~	~~0.024~~	~~0.058~~
~~^{97}Nb*~~	~~743~~	~~M4 $(\frac{1}{2}^-) \rightarrow (\frac{9}{2}^+)$~~	~~0.055~~	~~0.13~~
^{135}Xe*	526	M4 $(\frac{11}{2}^-) \rightarrow (\frac{3}{2}^+)$	0.0097	0.023
^{137}Ba*	662	M4 $(\frac{11}{2}^-) \rightarrow (\frac{3}{2}^+)$	0.0042	0.010

BIGSTICK can calculate the parameters of the branching ratio. However….

p/n orbits are different

too many nucleons

TEXONO Collaboration, hep-ex/0609001

Branching ratio

F. T. Avignone III, et al., PRD.37.618, 1988

gs = 0 (n (exp)) gs = 1 (n (BIGSTICK))

Nucleus	transition	ΔE [keV]	J	n (exp)	n (BIGSTICK)	beta	eta
Li7	M1	478	1/2- => 3/2-	1 => 0	2 => 1	1	-3.4 * 10^-3
Xe135	M4	526	11/2- => 3/2+	2 => 0			
Ba137	M4	662	11/2- => 3/2+	2 => 0			

$$\left(\frac{\Gamma_a}{\Gamma_\gamma}\right)_{\mathrm{MJ}} = \frac{1}{\pi\alpha}\frac{1}{1+\delta^2}\frac{J}{J+1}\left(\frac{|\vec{p}_a|}{|\vec{p}_\gamma|}\right)^{2J+1} \times \left(\frac{\boxed{g_{ann}}(1+\beta)}{(\mu_0 - 1/2)\beta + \mu_1 - \eta}\right)^2, \quad \delta \approx 0$$

$g_{ann}(\text{at left}) = g_{ann}(\text{in 1st slide}) \times GeV$

$g_{ann}(\text{at left})$ is dimensionless

$$\beta = \frac{\left\langle J_f \left|\left| \sum_{i=1}^{A} \sigma(i) \right|\right| J_i \right\rangle}{\left\langle J_f \left|\left| \sum_{i=1}^{A} \sigma(i)\tau_3(i) \right|\right| J_i \right\rangle}$$

$$\eta = -\frac{\left\langle J_f \left|\left| \sum_{i=1}^{A} l(i)\tau_3(i) \right|\right| J_i \right\rangle}{\left\langle J_f \left|\left| \sum_{i=1}^{A} \sigma(i)\tau_3(i) \right|\right| J_i \right\rangle}$$

$$p + n \to D + \gamma/a$$

$$\frac{\Gamma_a}{\Gamma_\gamma}(pn \to d\gamma) = \frac{1}{2\pi\alpha}\left(\frac{p_a}{p_\gamma}\right)^3\left(\frac{g_{ann}^1}{\mu_1}\right)^2$$

equivalently $\delta = \beta = \eta = 0, J = 1$

Experiments

- Beam dump: CCM, IsoDAR, PIP2BD, …
- Reactor: MINER at Texas A&M

MINER
Mitchell Institute Neutrino
Experiment at Reactor

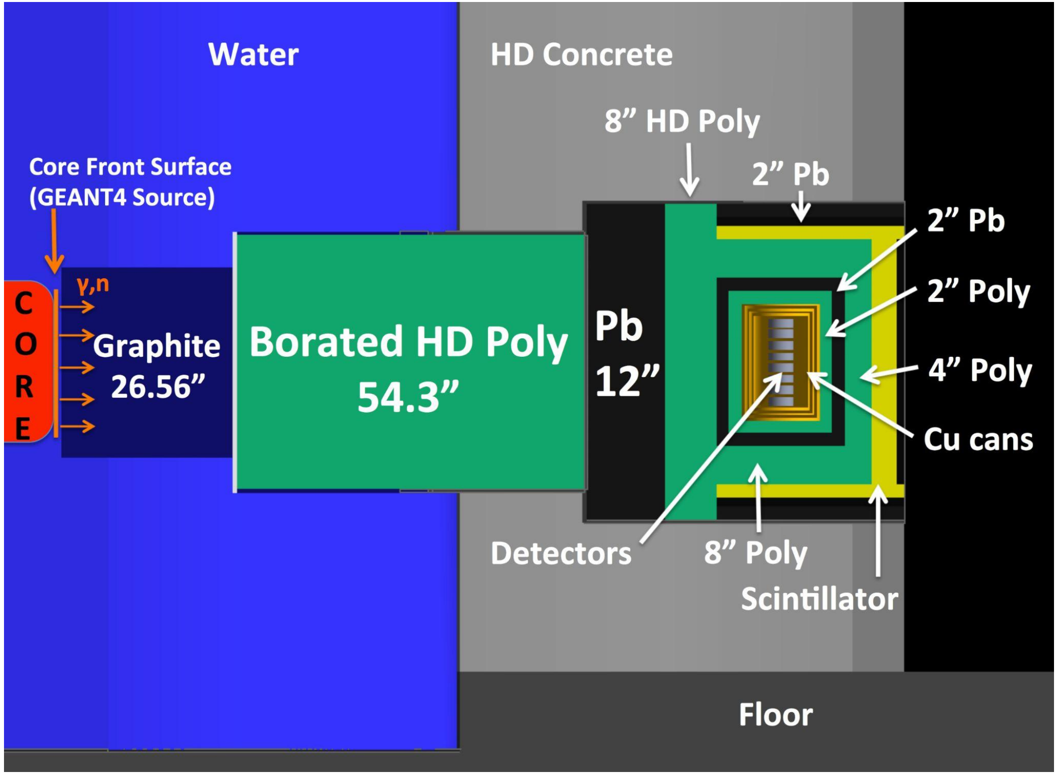

G. Agnolet et al., 1609.02066

MINER CsI detector

Background reduction: 10%
Exposure: 1 year
Detector threshold: 50 keV

Name	Mass [kg]	Area [m^2]	Length [m]	Distance [m]
1x1	3.547	0.0155	0.0508	4
3x3	31.923	0.0464	0.1524	4

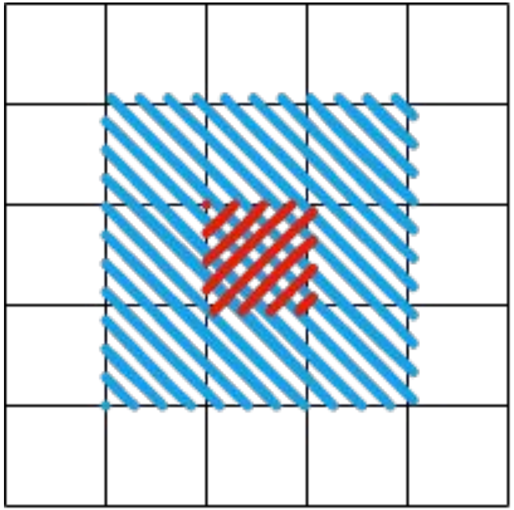

Detectors array
Blue: 3x3
Red: 1x1

MINER Background and photon flux

Window cuts on background
cut 1: 0.45-1.25 MeV
cut 2: 3.18-4.79 MeV

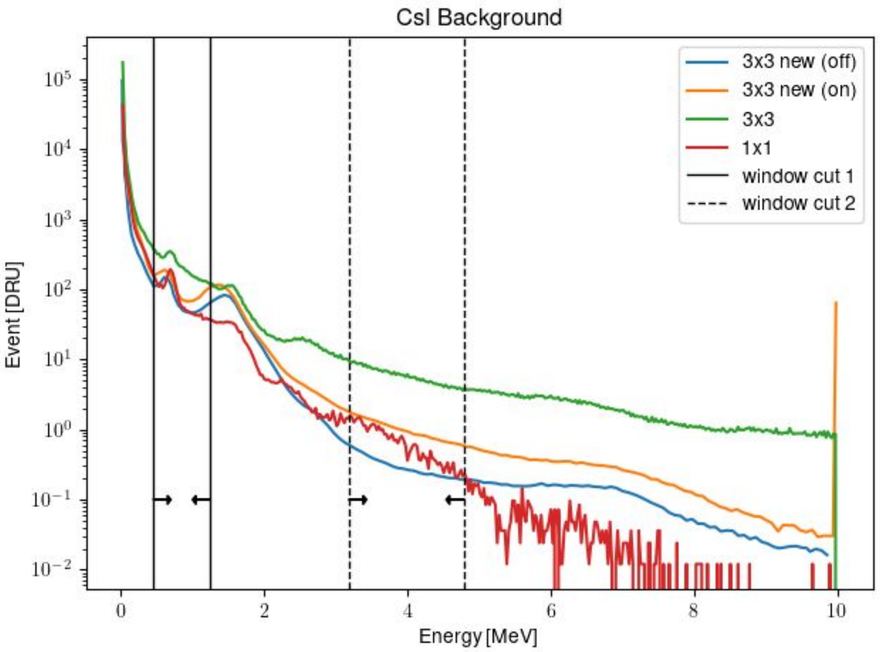

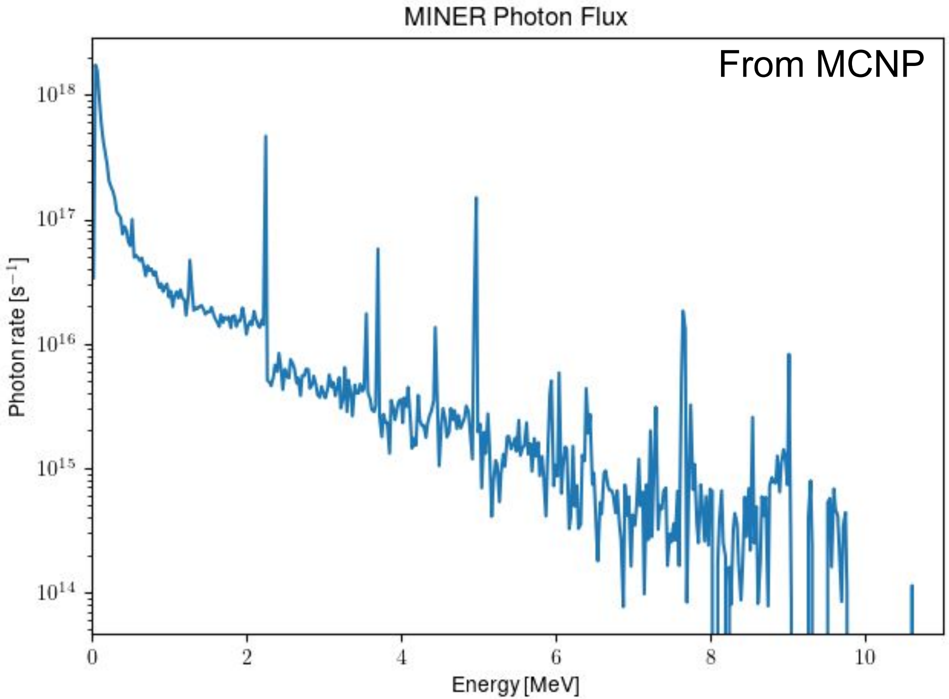

DRU = counts/kg/keV/day

BIGSTICK GT strength and cross section

$$\sigma_{\text{abs}}(E_a, \Delta_2) = \frac{g_A^2 \pi}{6(2J+1)} g_{ann}^2 \delta(E_a - E_r - \Delta_2)\, p_a \left| \langle J_f || \sum_{i=1}^{A} \frac{1}{2} \hat{\sigma}_i \hat{\tau}_0 || J_i \rangle \right|^2$$

$$\sigma_{\text{abs}}(E_a) = \sum_{\Delta_2 \leq E_a} \sigma_{\text{abs}}(E_a, \Delta_2)$$

$$\Delta_2 = \text{excitation energy}$$

BIGSTICK output (Cs133)

Energy	Strength	
-300.05300	0.00020	ground state
-300.01663	0.00471	
-299.81764	0.00114	
-299.69193	0.00000	
-299.57699	0.00000	
-299.50052	0.00000	
-299.45278	0.00314	
-299.41415	0.00000	
-299.39827	0.00013	
-299.33202	0.00419	
-299.27586	0.00008	
-299.21456	0.00368	
-299.18414	0.00000	

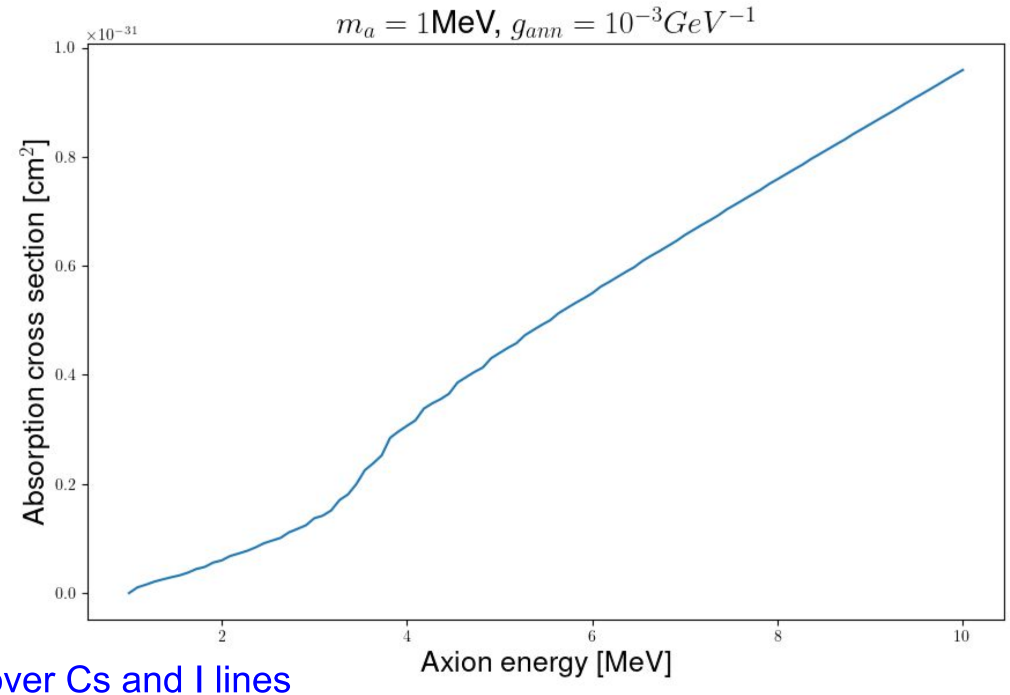

sum over Cs and I lines

Nuclear lines in PIP2BD

Nucleus	Energy [MeV]	per 10^5 POT
Li7	0.435	887.041
N15	5.266	13.836
O16	2.774	13.836

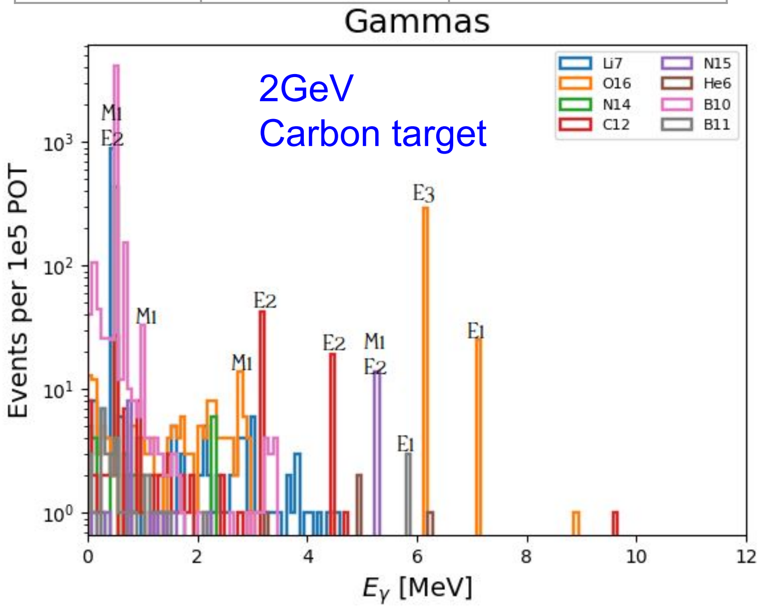

There are too many nuclei, but most of them are not matched with experiment data. Ni60 seems to be the best match

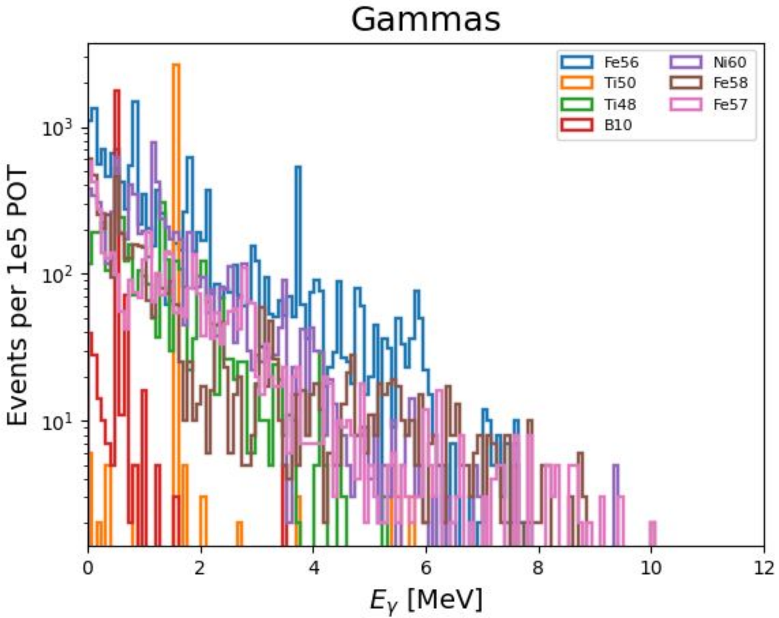

Source: nuclear deexcitation
Detection: nuclear absorption

*axions don't decay

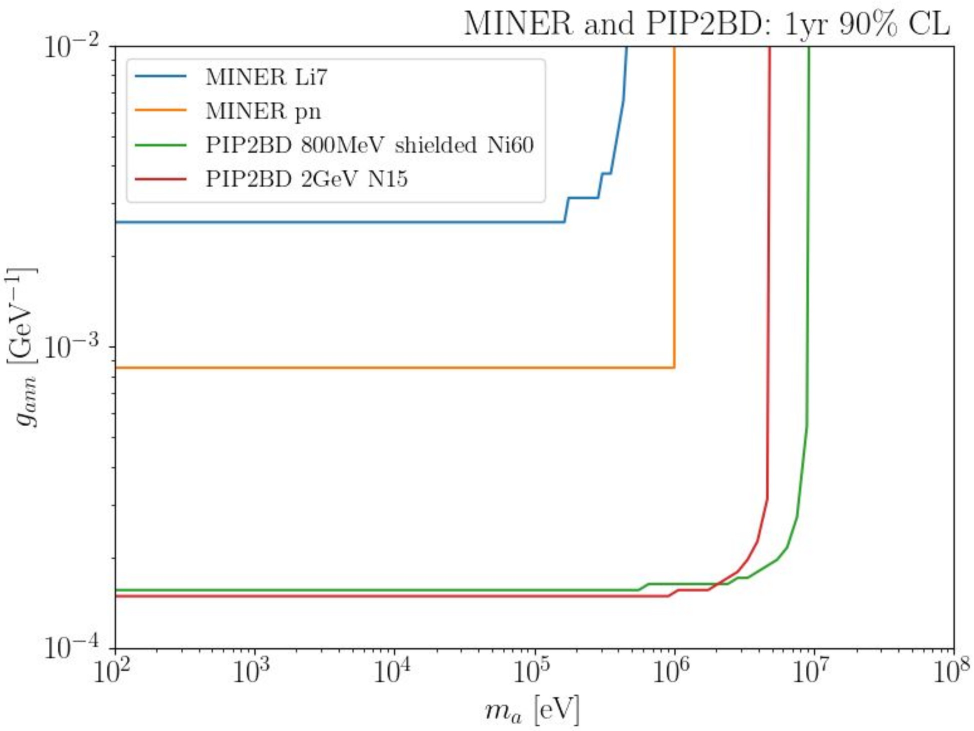

PIP2BD
100t LAr, 1yr exposure
1e23 total POT
100 bkg reduction

Lines:

- Ni60 9.38MeV (800MeV beam, shielded target)
- N15 5.266MeV (2GeV beam, C target)

MINER
32kg CsI, 1yr exposure
No bkg reduction

Lines:

- Li7 478keV
- pn 2230keV

Source: primakoff AND/OR nuclear
Detection: inv. primakoff, decay, absorption

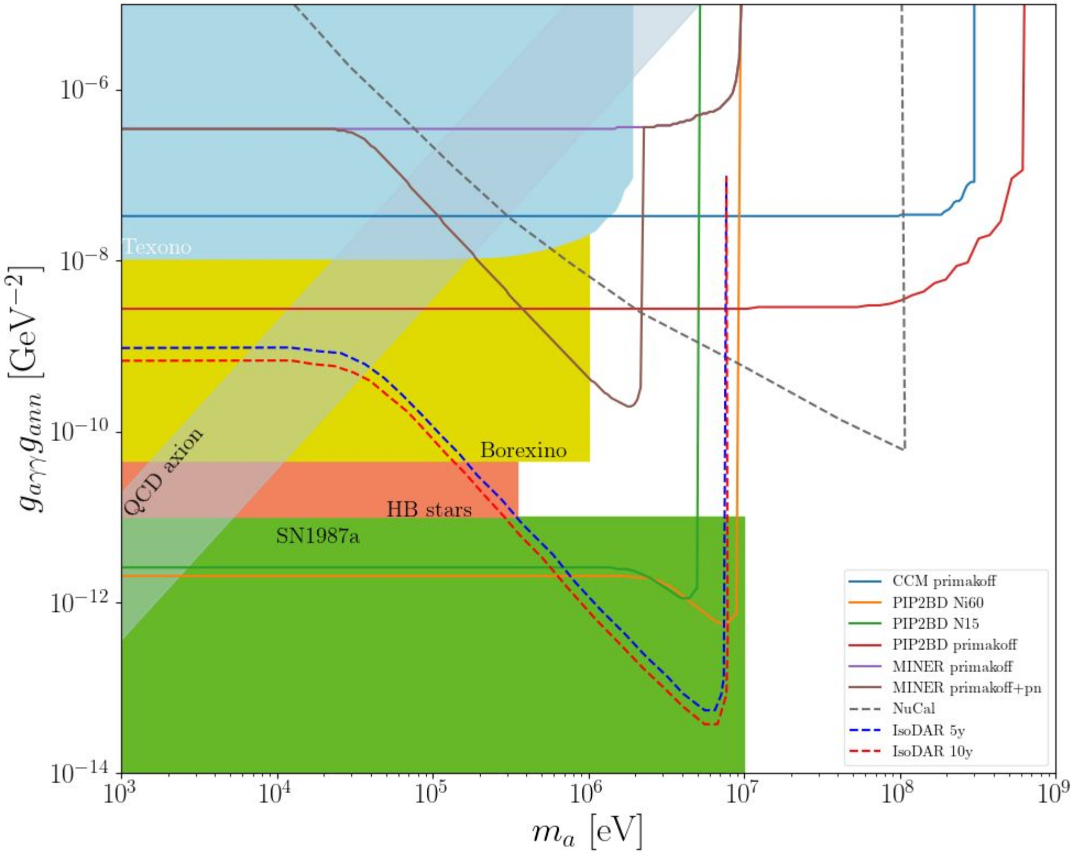

IsoDAR

8e24 POT per 5 yr
2.26kton liquid scintillator
17 meter away from target

Nucleus	Energy in MeV	Type	β	η
Fe57	7.606	M1	0.7071	-0.3111
Li8	1.009	M1	1	-0.0260
Li8	2.053	M1	1	-0.1034
O15	5.281	M2	1	0.5

L. Waites et al., 2207.13659

Conclusion

- We calculate the inelastic cross-section and event rates for DM/WIMP/axion nucleus scattering.
- Gamow-Teller transitions in long wavelength limit dominate the cross section.
- With inelastic scattering, we explore new region on the parameter space.
- We can remove most of the neutrino background efficiently with prompt timing cut in DM search in beam dump experiments

Next steps

- Search in MicroBoone and SBND
- Apply efficiency to have better estimation of the search

Backup slides

The shaded region in DM sensitivities plots

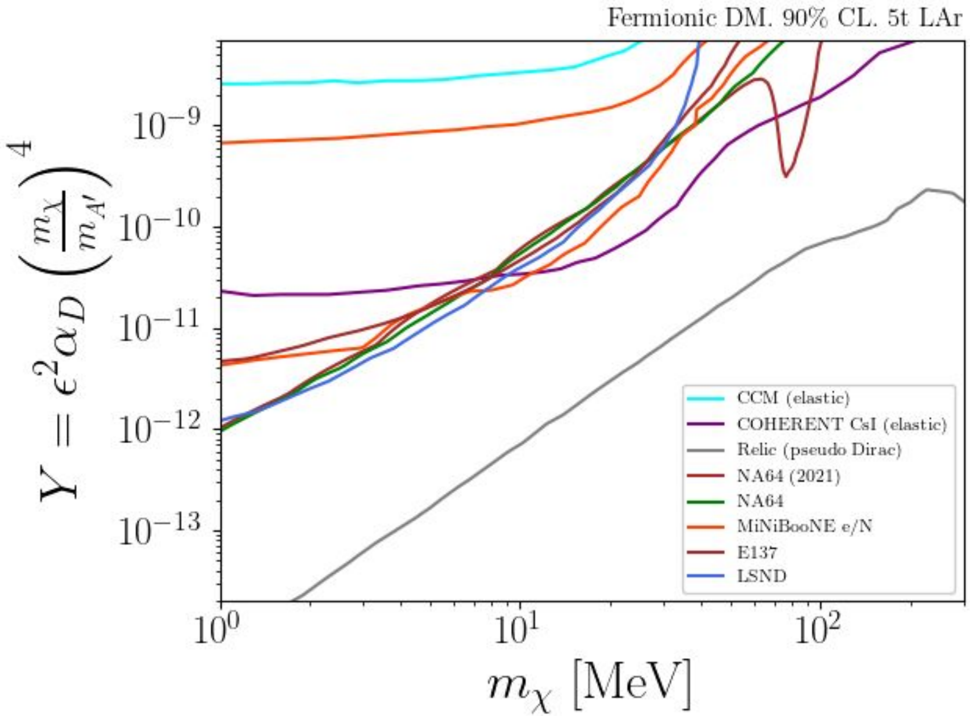

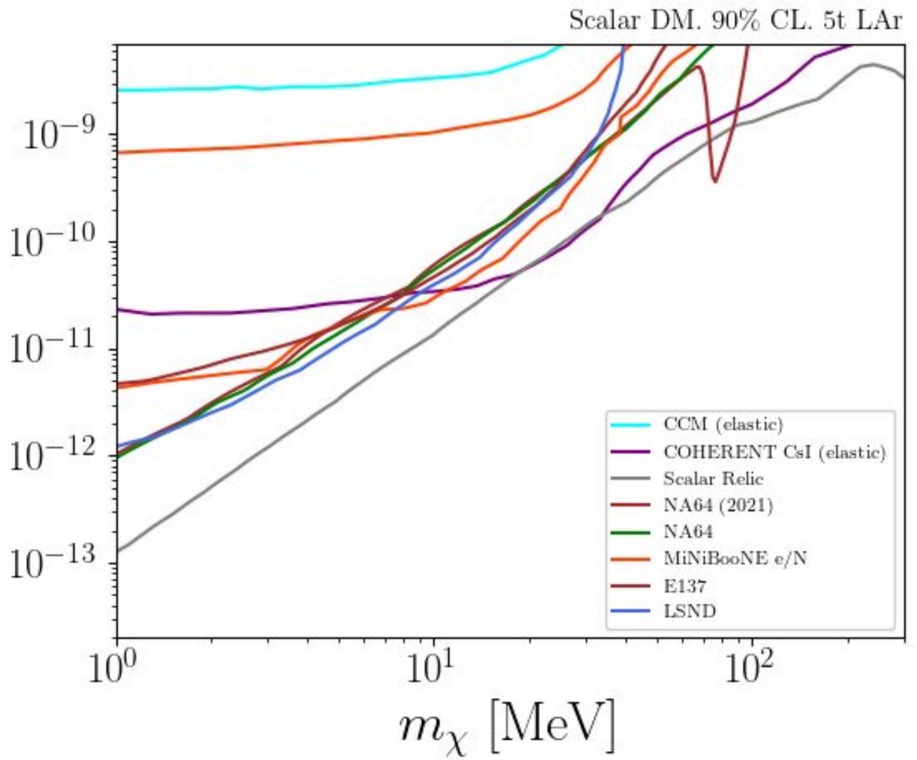

Multipole expansion (Standard Model)

Current-current interaction in Hamiltonian

Lepton current

Nucleus current

$$\langle f|\hat{H}_W|i\rangle = -\frac{G}{\sqrt{2}} l_\mu \int d^3x\, e^{-i\mathbf{q}\cdot\mathbf{x}} \langle f|\hat{\mathcal{J}}_\mu(\mathbf{x})|i\rangle$$
$$= -\frac{G}{\sqrt{2}} \int d^3x\, e^{-i\mathbf{q}\cdot\mathbf{x}} [\mathbf{l}\cdot\boldsymbol{\mathcal{J}}(\mathbf{x})_{fi} - l_0 \mathcal{J}_0(\mathbf{x})_{fi}]$$

$$\mathbf{e}^\dagger_{\mathbf{q}\lambda} e^{-i\mathbf{q}\cdot\mathbf{x}} = -\sum_{J\geq 1}^{\infty} \sqrt{2\pi(2J+1)}(-i)^J \left\{\lambda j_J(\kappa x)\boldsymbol{\mathcal{Y}}^{-\lambda}_{JJ1} + \frac{1}{\kappa}\nabla\times\left[j_J(\kappa x)\boldsymbol{\mathcal{Y}}^{-\lambda}_{JJ1}\right]\right\}$$

$$;\ \text{for } \lambda = \pm 1$$

$$\mathbf{e}^\dagger_{\mathbf{q}0} e^{-i\mathbf{q}\cdot\mathbf{x}} = \frac{i}{\kappa}\sum_{J\geq 0}^{\infty} \sqrt{4\pi(2J+1)}(-i)^J \nabla[j_J(\kappa x) Y_{J0}]$$

Spatial decomposition

$$\langle f|j^{\text{lept}}_\mu(\mathbf{x})|i\rangle = l_\mu e^{-i\mathbf{q}\cdot\mathbf{x}}$$
$$\mathbf{l} = \sum_{\lambda=0,\pm 1} l_\lambda \mathbf{e}^\dagger_\lambda$$

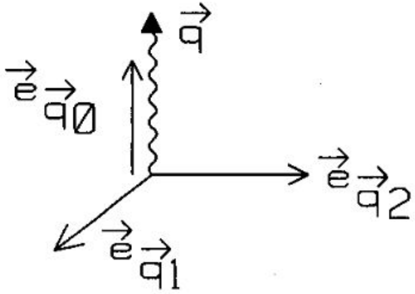

J. D. Walecka, 2004

Multipole expansion (Standard Model)

$$\langle f|\hat{H}_{\mathrm{W}}|i\rangle = \frac{-G}{\sqrt{2}}\langle f| \Bigg\{ -\sum_{J\geq 1}\sqrt{2\pi(2J+1)}(-i)^J \sum_{\lambda=\pm 1} l_\lambda \left[\lambda \hat{\mathcal{T}}^{\mathrm{mag}}_{J-\lambda}(\kappa) + \hat{\mathcal{T}}^{\mathrm{el}}_{J-\lambda}(\kappa)\right]$$

$$+\sum_{J\geq 0}\sqrt{4\pi(2J+1)}(-i)^J \left[l_3 \hat{\mathcal{L}}_{J0}(\kappa) - l_0 \hat{\mathcal{M}}_{J0}(\kappa)\right] \Bigg\} |i\rangle$$

Multipole Operators

$$\hat{\mathcal{M}}_{JM}(\kappa) \equiv \hat{M}_{JM} + \hat{M}^5_{JM} = \int d^3x [j_J(\kappa x) Y_{JM}(\Omega_x)] \hat{\mathcal{J}}_0(\mathbf{x})$$

$$\hat{\mathcal{L}}_{JM}(\kappa) \equiv \hat{L}_{JM} + \hat{L}^5_{JM} = \frac{i}{\kappa}\int d^3x \{\nabla [j_J(\kappa x) Y_{JM}(\Omega_x)]\} \cdot \hat{\boldsymbol{\mathcal{J}}}(\mathbf{x})$$

$$\hat{\mathcal{T}}^{\mathrm{el}}_{JM}(\kappa) \equiv \hat{T}^{\mathrm{el}}_{JM} + \hat{T}^{\mathrm{el5}}_{JM} = \frac{1}{\kappa}\int d^3x [\nabla \times j_J(\kappa x) \boldsymbol{\mathcal{Y}}^M_{JJ1}(\Omega_x)] \cdot \hat{\boldsymbol{\mathcal{J}}}(\mathbf{x})$$

$$\hat{\mathcal{T}}^{\mathrm{mag}}_{JM}(\kappa) \equiv \hat{T}^{\mathrm{mag}}_{JM} + \hat{T}^{\mathrm{mag5}}_{JM} = \int d^3x [j_J(\kappa x) \boldsymbol{\mathcal{Y}}^M_{JJ1}(\Omega_x)] \cdot \hat{\boldsymbol{\mathcal{J}}}(\mathbf{x})$$

J. D. Walecka, 2004

Multipole operator and response function

Multipole Operators

Response functions

$$\mathcal{M} = \mathcal{M}_{LM} + \mathcal{M}^5_{LM} = \left\{ F_1^N M_L^M + \frac{\mathbf{q}^2}{4m_N^2}(F_1^N + 2F_2^N)(\Phi_L^{''M} - \frac{1}{2}M_{LM}) \right\} + \left\{ -i\frac{|\mathbf{q}|}{m_N} G_A^N \left[\Omega_L^M + \frac{1}{2}\Sigma_L^{''M} \right] \right\}$$

$$\mathcal{L} = \mathcal{L}_{LM} + \mathcal{L}^5_{LM} = \left\{ \frac{q^0}{|\mathbf{q}|}\mathcal{M} \right\} + \left\{ i \left[G_A^N(1 - \frac{\mathbf{q}^2}{8m_N^2}) - \frac{\mathbf{q}^2}{4m_N^2} G_P^N \right] \Sigma_L^{''M} \right\}$$

$$\mathcal{T}^{el} = \mathcal{T}^{el}_{LM} + \mathcal{L}^{el5}_{LM} = \left\{ \frac{|\mathbf{q}|}{m_N} \left[F_1^N \Delta_L^{'M} + \frac{F_1^N + F_2^N}{2}\Sigma_L^M \right] \right\} + \left\{ iG_A^N(1 - \frac{\mathbf{q}^2}{8m_N^2})\Sigma_L^{'M} \right\}$$

$$\mathcal{T}^{mag} = \mathcal{T}^{mag}_{LM} + \mathcal{L}^{mag5}_{LM} = \left\{ -i\frac{|\mathbf{q}|}{m_N} \left[F_1^N \Delta_L^M - \frac{F_1^N + F_2^N}{2}\Sigma_L^{'M} \right] \right\} + \left\{ G_A^N(1 - \frac{\mathbf{q}^2}{8m_N^2})\Sigma_L^M \right\}$$

Multipole expansion (Standard Model)

$$\frac{1}{(2J_i+1)}\sum_{M_i}\sum_{M_f}|\langle f|\hat{H}_{\rm W}|i\rangle|^2 = \frac{G^2}{2}\frac{4\pi}{(2J_i+1)}\times$$

$$\left\{\sum_{J\geq 1}\left[\frac{1}{2}(\mathbf{l}\cdot\mathbf{l}^* - l_3 l_3^*)\left(|\langle J_f||\hat{\mathcal{T}}_J^{\rm mag}||J_i\rangle|^2 + |\langle J_f||\hat{\mathcal{T}}_J^{\rm el}||J_i\rangle|^2\right)\right.\right.$$

$$\left.-\frac{i}{2}(\mathbf{l}\times\mathbf{l}^*)_3\left(2\,{\rm Re}\langle J_f||\hat{\mathcal{T}}_J^{\rm mag}||J_i\rangle\langle J_f||\hat{\mathcal{T}}_J^{\rm el}||J_i\rangle^*\right)\right]$$

$$+\sum_{J\geq 0}\left[l_3 l_3^*|\langle J_f||\hat{\mathcal{L}}_J||J_i\rangle|^2 + l_0 l_0^*|\langle J_f||\hat{\mathcal{M}}_J||J_i\rangle|^2\right.$$

$$\left.\left.-2\,{\rm Re}\left(l_3 l_0^*\langle J_f||\hat{\mathcal{L}}_J||J_i\rangle\langle J_f||\hat{\mathcal{M}}_J||J_i\rangle^*\right)\right]\right\}$$

See details at the book Theoretical Nuclear and Subnuclear Physics (2ed) by Walecka

Cross section

$$\left(\frac{d\sigma}{d\Omega}\right)_{\substack{\nu\\ \bar{\nu}}}^{\rm ERL} = \frac{G^2\varepsilon^2}{2\pi^2}\frac{4\pi}{2J_i+1}\left\{\cos^2\frac{\theta}{2}\sum_{J=0}^{\infty}|\langle J_f||\hat{\mathcal{M}}_J - \frac{q_0}{|\mathbf{q}|}\hat{\mathcal{L}}_J||J_i\rangle|^2\right.$$

$$+\left[\frac{q_\mu^2}{2\mathbf{q}^2}\cos^2\frac{\theta}{2}+\sin^2\frac{\theta}{2}\right]\sum_{J=1}^{\infty}\left[|\langle J_f||\hat{\mathcal{T}}_J^{\rm mag}||J_i\rangle|^2 + |\langle J_f||\hat{\mathcal{T}}_J^{\rm el}||J_i\rangle|^2\right]$$

$$\left.\mp\frac{\sin\theta/2}{|\mathbf{q}|}\sqrt{q_\mu^2\cos^2\frac{\theta}{2}+\mathbf{q}^2\sin^2\frac{\theta}{2}}\sum_{J=1}^{\infty}2{\rm Re}\left[\langle J_f||\hat{\mathcal{T}}_J^{\rm mag}||J_i\rangle\langle J_f||\hat{\mathcal{T}}_J^{\rm el}||J_i\rangle^*\right]\right\}$$

J. D. Walecka, 2004

Inel DM scattering cross section

$$\frac{d\sigma_{inel}^{DM}}{dE_r} = \frac{2e^2\epsilon^2 g_D^2 E'^2_\chi}{p_\chi p'_\chi (2m_N E_r + m_{A'}^2)^2} \frac{m_N}{2\pi} \frac{4\pi}{2J+1}$$

$$\times \sum_{s_i, s_f} \vec{l} \cdot \vec{l}^* \frac{g_A^2}{12\pi} |\langle J_f || \sum_{i=1}^{A} \frac{1}{2} \hat{\sigma}_i \hat{\tau}_0 || J_i \rangle|^2$$

Rewrite in scattering angle with

$$\frac{d\sigma}{dE_r} = \frac{d\sigma}{d\Omega}\frac{d\Omega}{dE_r} = 2\pi \frac{d\sigma}{d\Omega}\frac{m_N}{p_\chi p'_\chi} = \frac{d\sigma}{d\cos\theta}\frac{m_N}{p_\chi p'_\chi}$$

$$\frac{d\sigma_{inel}^{DM}}{d\cos\theta} = \frac{2e^2\epsilon^2 g_D^2 E'^2_\chi}{(2m_N E_r + m_{A'}^2)^2} \frac{1}{2\pi} \frac{4\pi}{2J+1}$$

$$\times \sum_{s_i, s_f} \vec{l} \cdot \vec{l}^* \frac{g_A^2}{12\pi} |\langle J_f || \sum_{i=1}^{A} \frac{1}{2} \hat{\sigma}_i \hat{\tau}_0 || J_i \rangle|^2$$

Raw Discrete Strength Lines

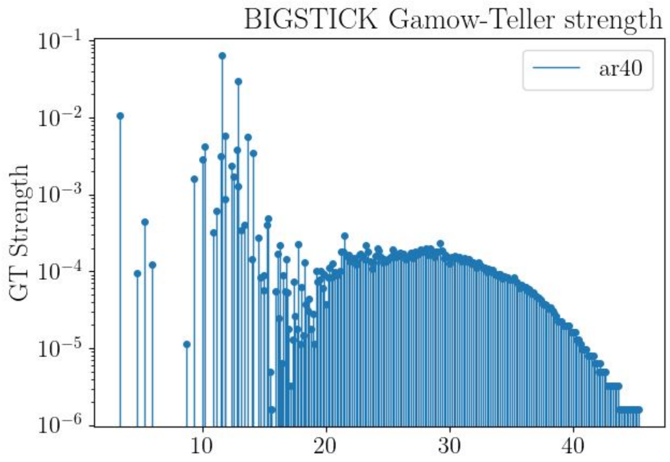

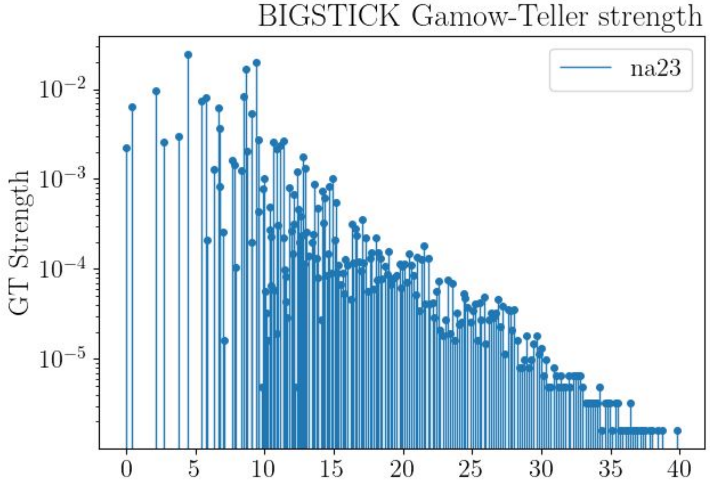

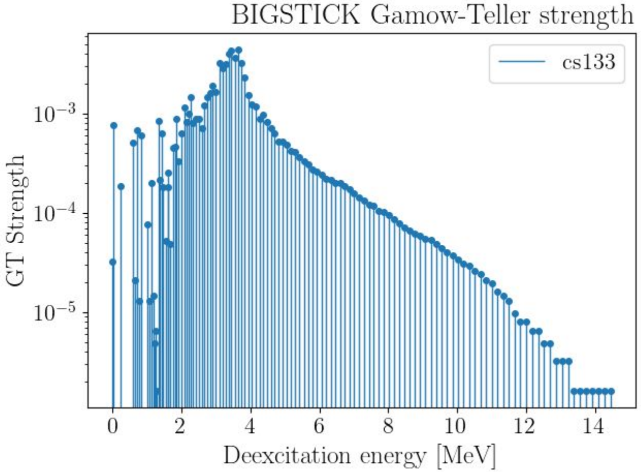

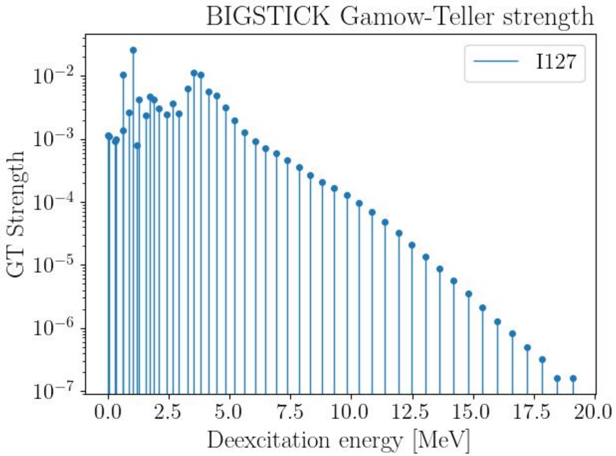

Convolution Plots

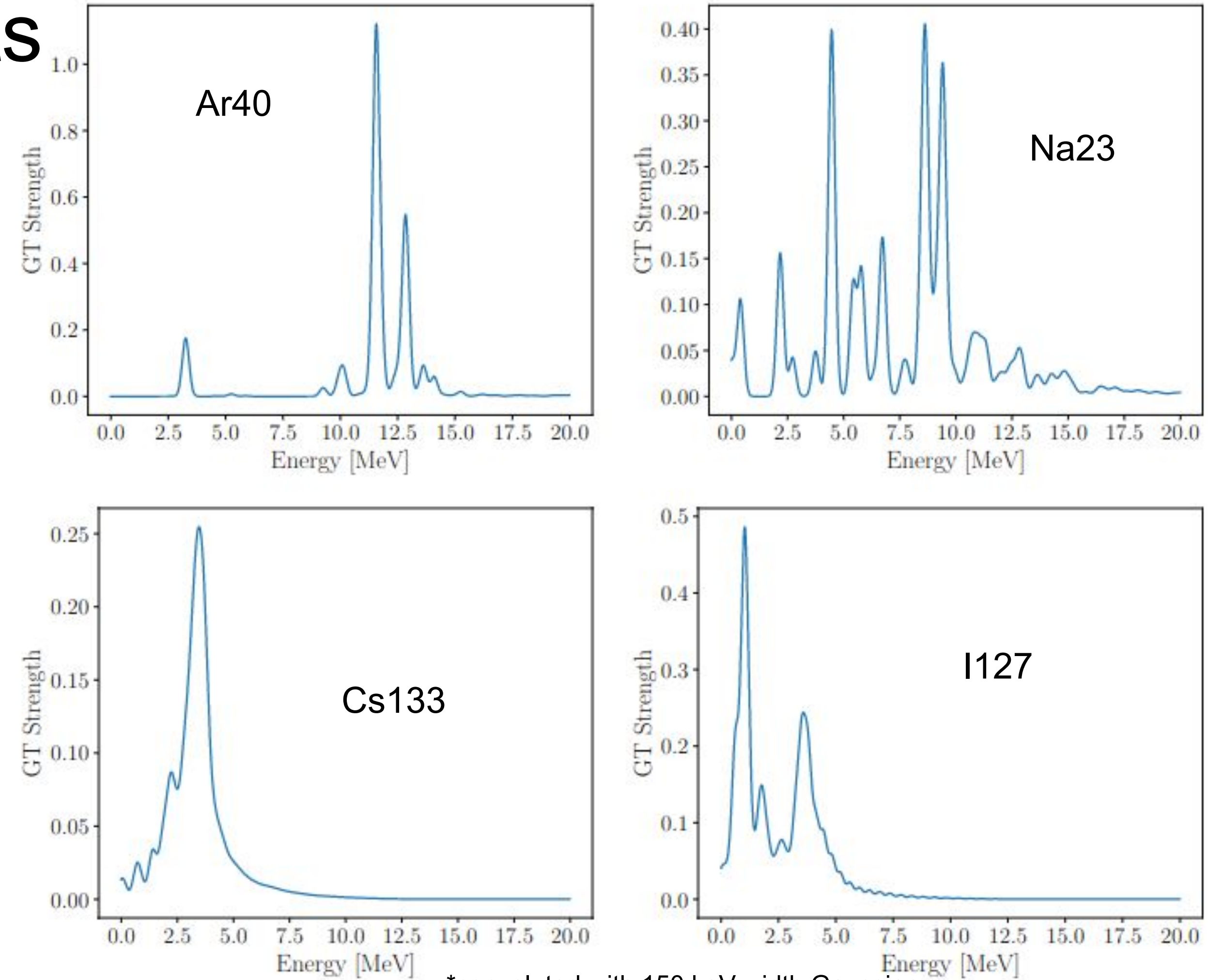

*convoluted with 150 keV width Gaussian

Inelastic neutrino-nucleus scattering

Similar to DM scattering, GT also dominates

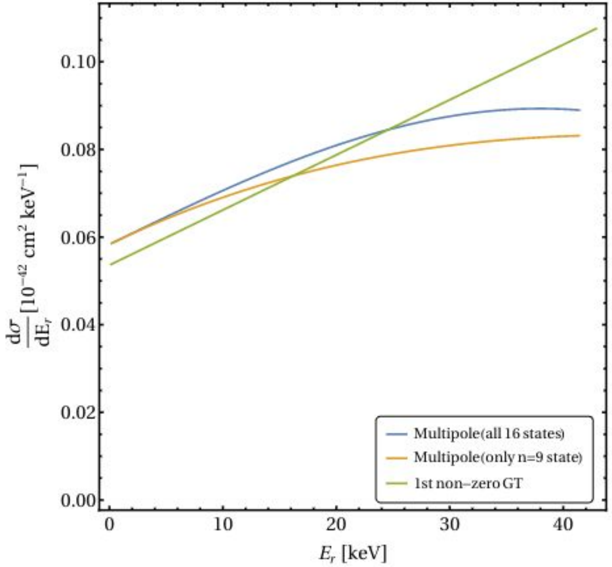

$$\sigma_\nu^{GT} \approx \frac{G_f^2 g_A^2}{\pi(2J+1)}(E_\nu - \Delta E)^2 |\langle J_f || \sum_{i=1}^{A} \frac{1}{2}\hat{\sigma_i}\hat{\tau_0} || J_i \rangle|^2 .$$

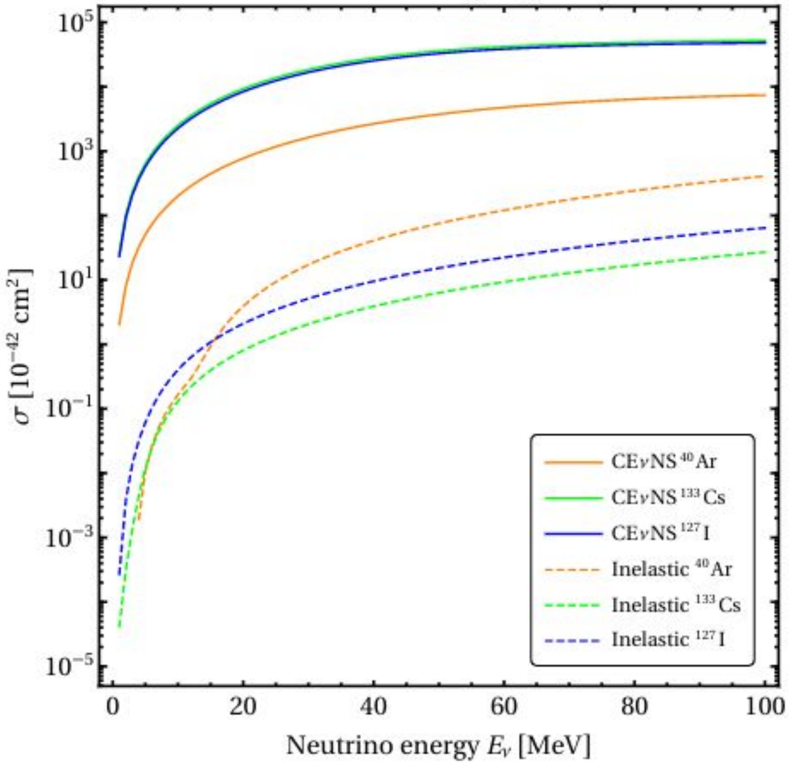

Events

Scattering	Experiment	Elastic	Inelastic	Ratio
ν-^{40}Ar	COHERENT	2.27×10^2	3.15	7.21×10
ν-^{40}Ar	CCM	1.91×10^4	2.65×10^2	7.21×10
ν-^{133}Cs	COHERENT	1.16×10^3	1.52×10^{-2}	7.65×10^3
ν-^{127}I	COHERENT	1.06×10^3	3.75×10^{-1}	2.81×10^3

GT strength for neutrino scattering

30MeV nu energy

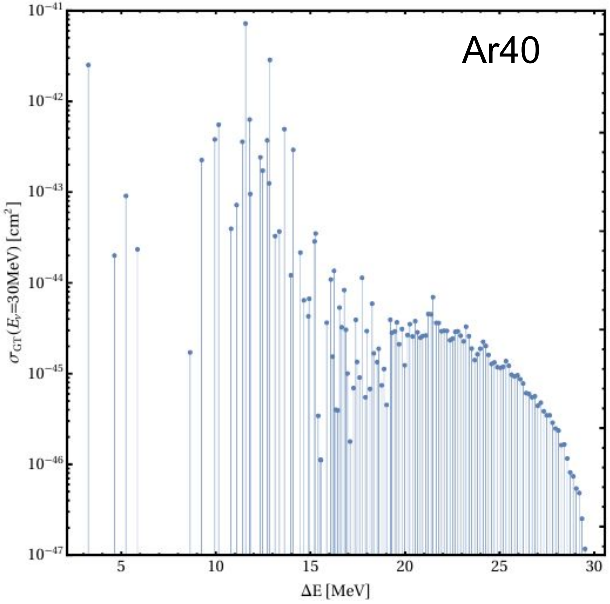

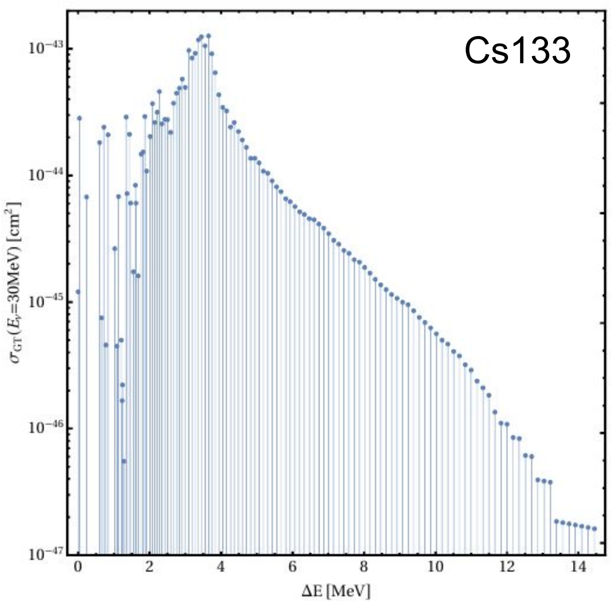

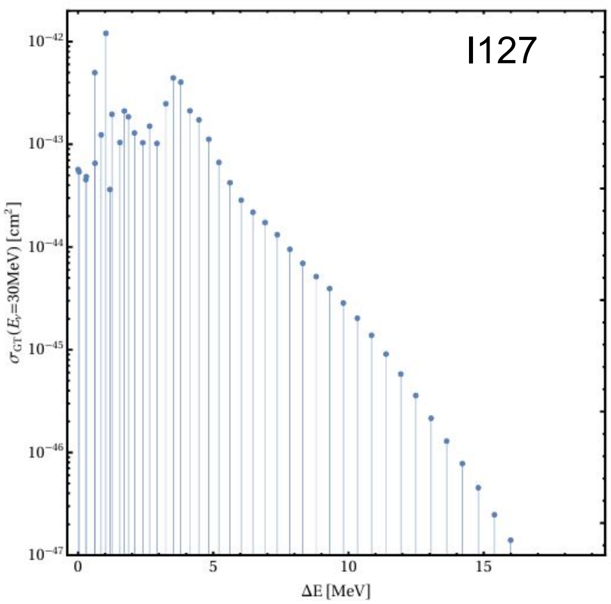

GT strength for neutrino scattering

30MeV nu energy
150 keV width Gaussian

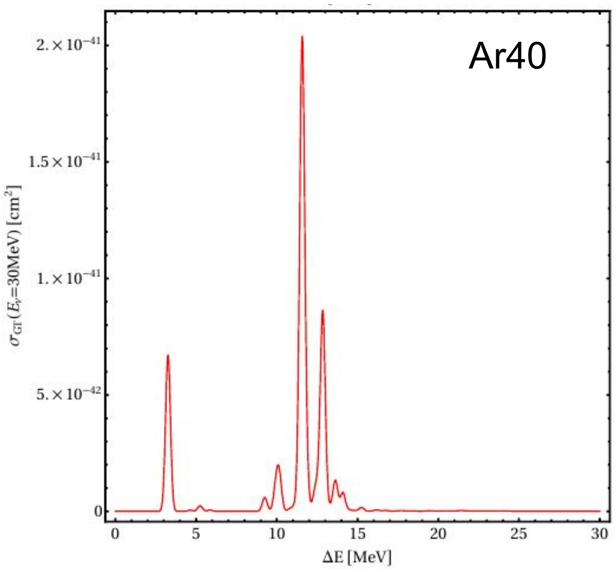

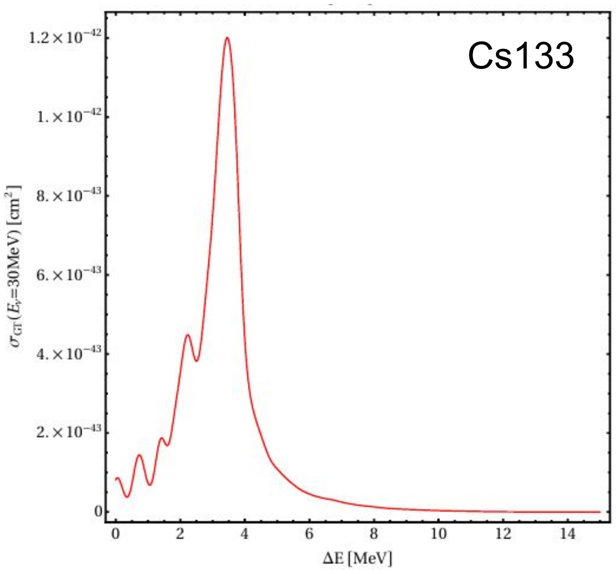

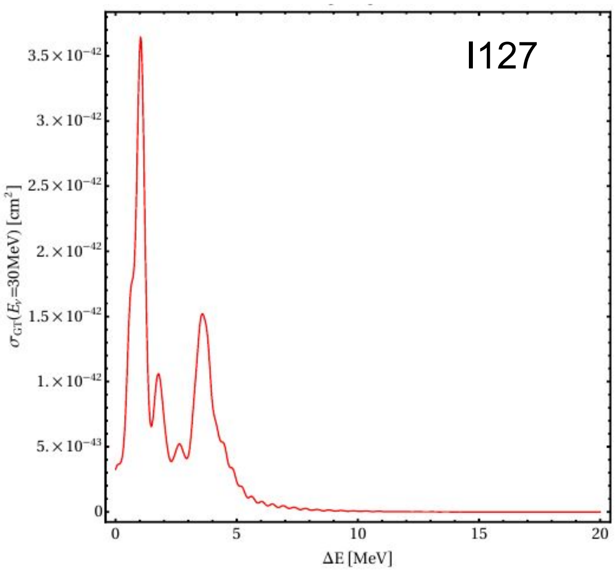

BIGSTICK ground state to ground state comparing to Helm form factor

MPD = multipole decomposition

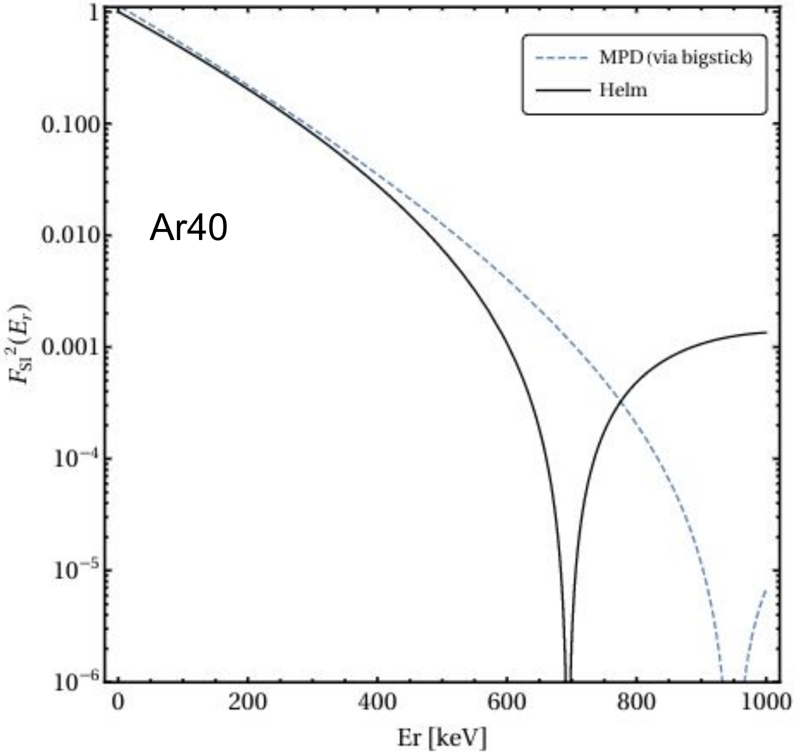

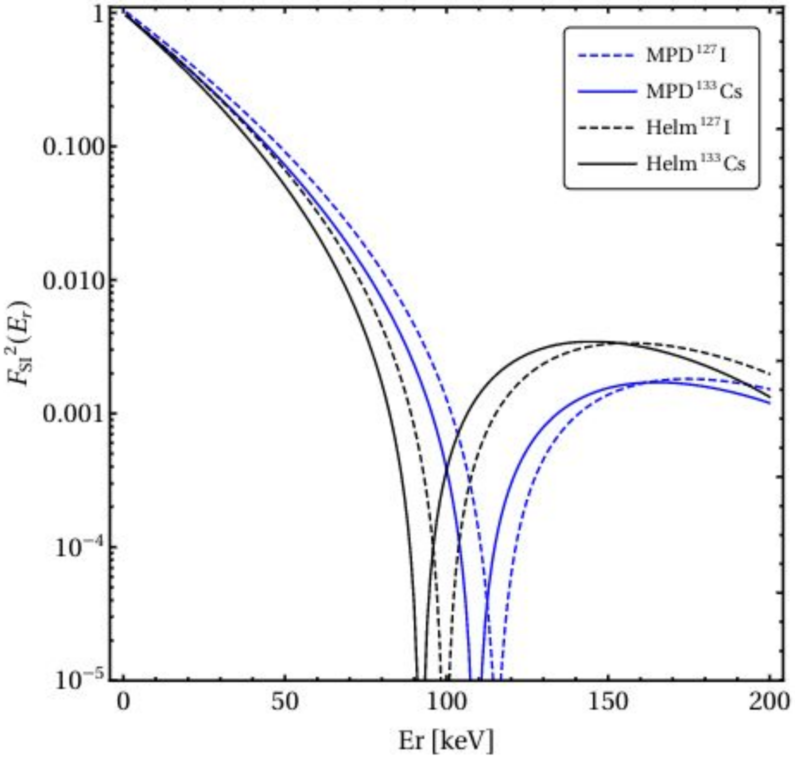

M lines from GEANT

PIP2BD

800MeV Be

Nucleus	Energy [MeV]	per 10^5 POT
Li7	0.435	141.2

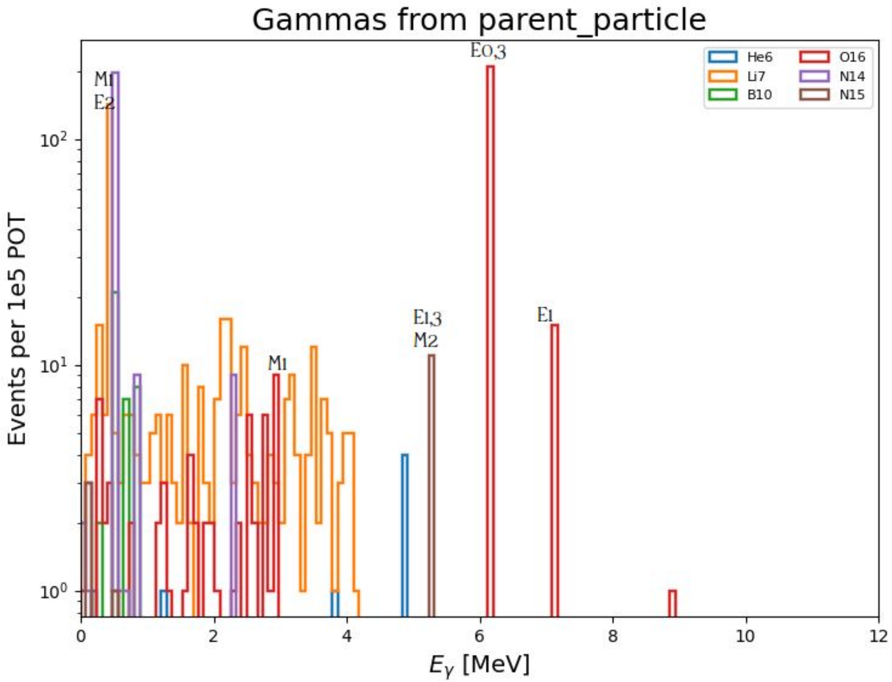

2GeV Be

Nucleus	Energy [MeV]	per 10^5 POT
Li7	0.435	222.54
N15	5.266	11.89

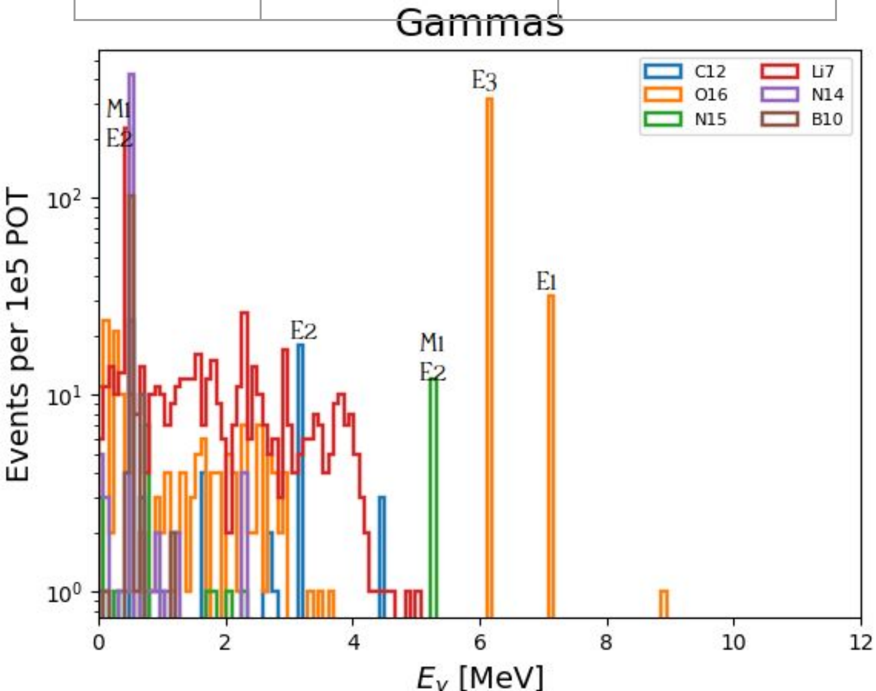

PIP2BD

Nucleus	Energy [MeV]	per 10^5 POT
Li7	0.435	465.8
N15	2.29	3.974
O16	2.774	13.836
B10	1	21.675

800MeV C

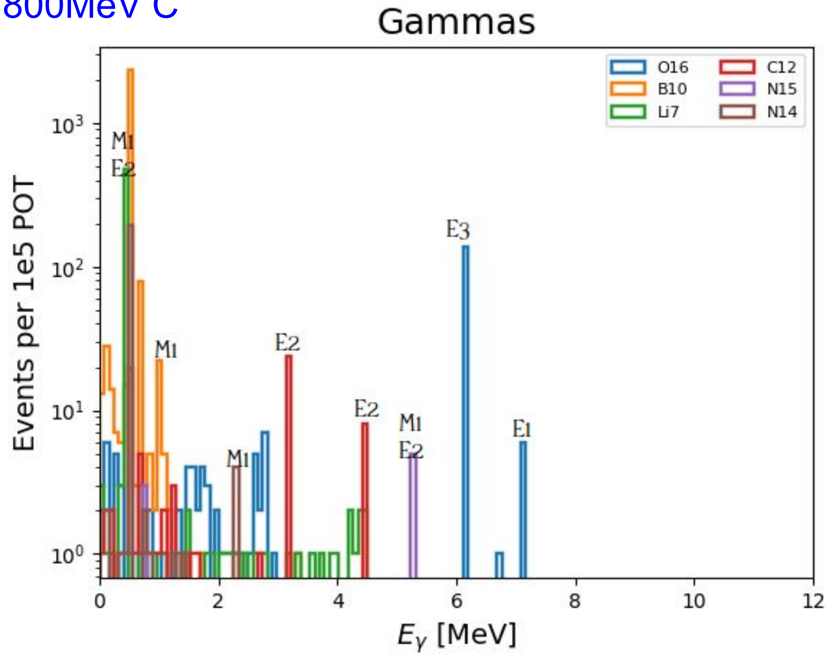

2GeV C

Nucleus	Energy [MeV]	per 10^5 POT
Li7	0.435	887.041
N15	5.266	13.836
O16	2.774	13.836
B10	1	32.79

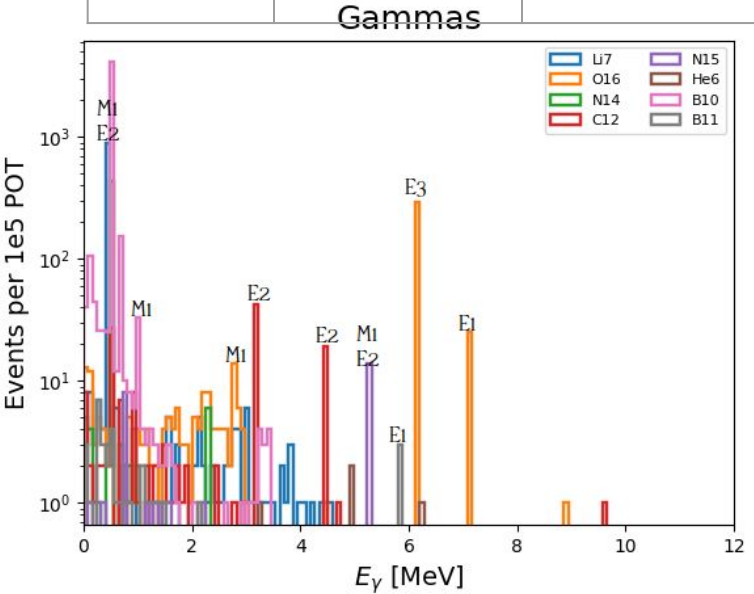

BIGSTICK energy level and spin

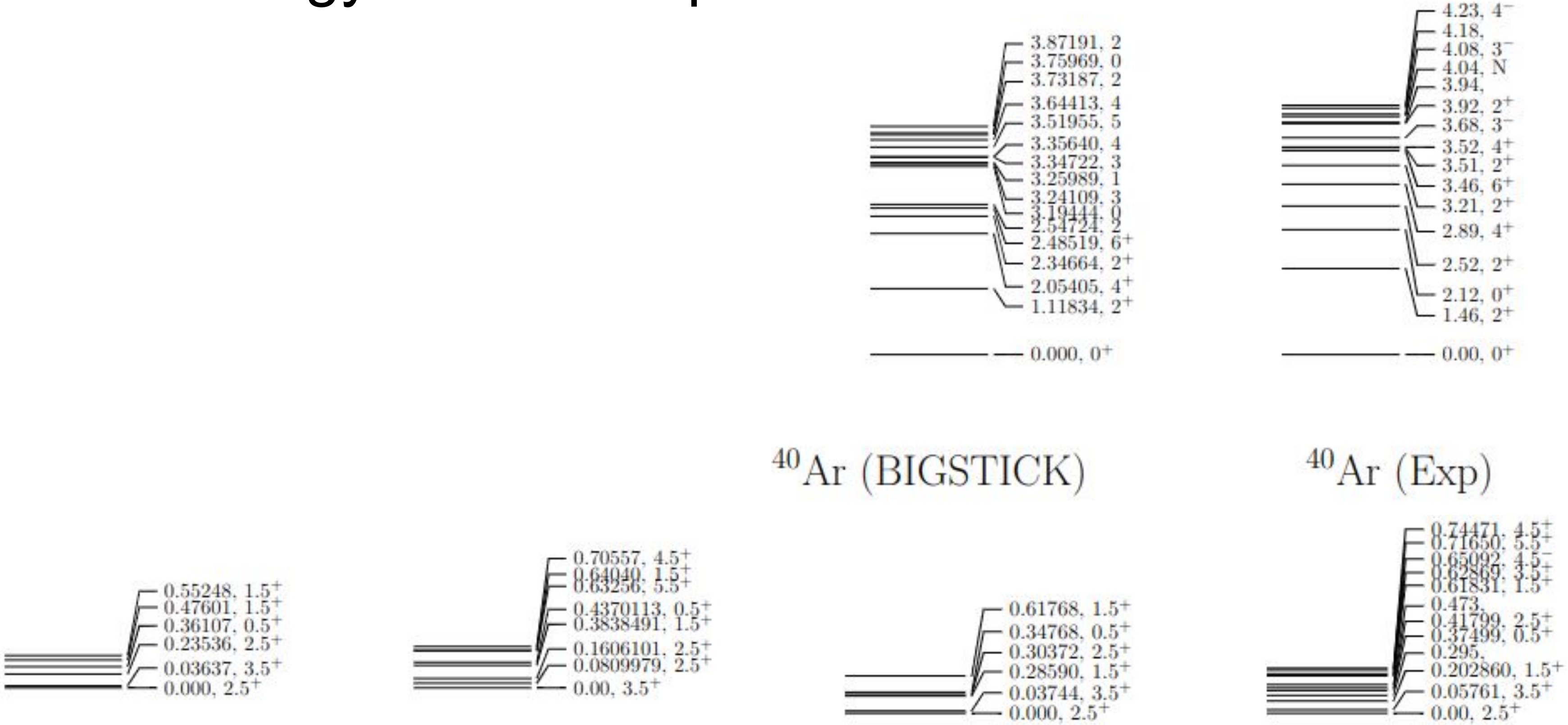

^{40}Ar (BIGSTICK)

^{40}Ar (Exp)

^{133}Cs (BIGSTICK)

^{133}Cs (Exp)

^{127}I (BIGSTICK)

^{127}I (Exp)

BIGSTICK nuclear magnetic moments

in keV

Nucleus	level n	J^π	μ	Expt.	E_x	Expt.
^{127}I	1	$5/2^+$	3.851	2.813	0	0
	2	$7/2^+$	3.007	2.54	37.44	57.61
	3	$3/2^+$	0.9155	0.97	285.9	202.86
^{133}Cs	1	$7/2^+$	3.007	2.582	0	0
	2	$5/2^+$	3.851	3.45	36.37	80.9979
	3	$5/2^+$	2.5849	2.0	235.36	160.6101
^{40}Ar	1	0^+	0	N/A	0	0
	2	2^+	0	-0.04	1118.33	1460.85

Source: Li7 (M1 478keV) / pn (M1 2230keV)
Detection: nuclear absorption

MINER

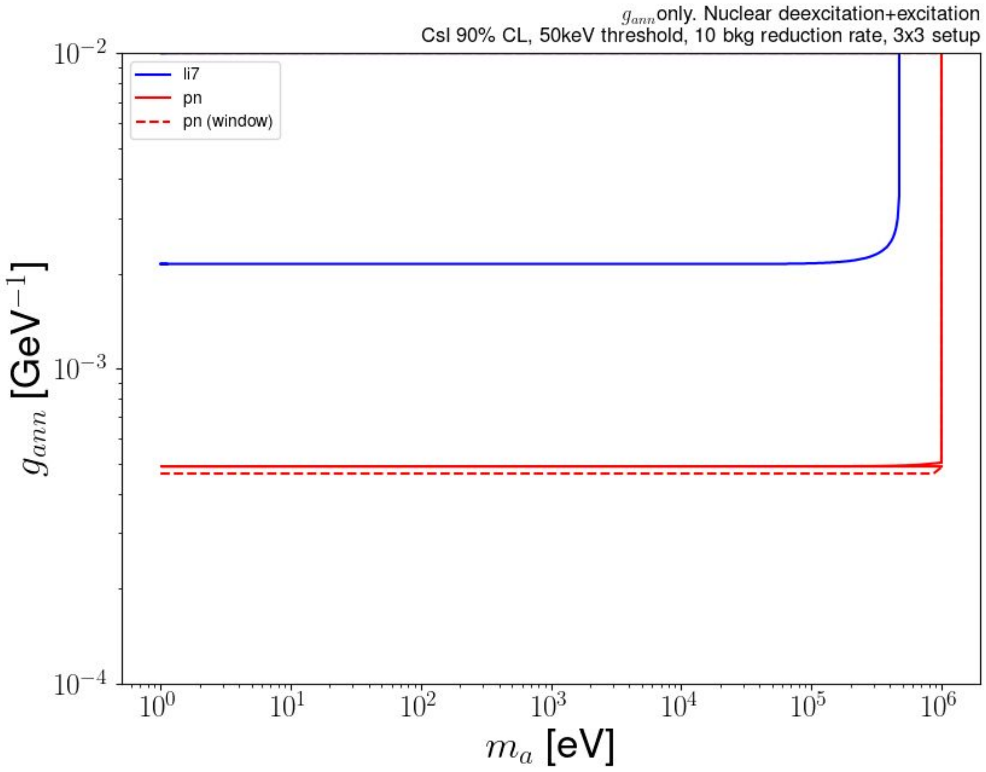

*axions don't decay

Energy window: 0.45-1.25MeV
Li7 is skipped because it doesn't have enough of bins

Source: Ni60 9.38MeV / N15 5.266MeV
Detection: nuclear absorption

PIP2BD

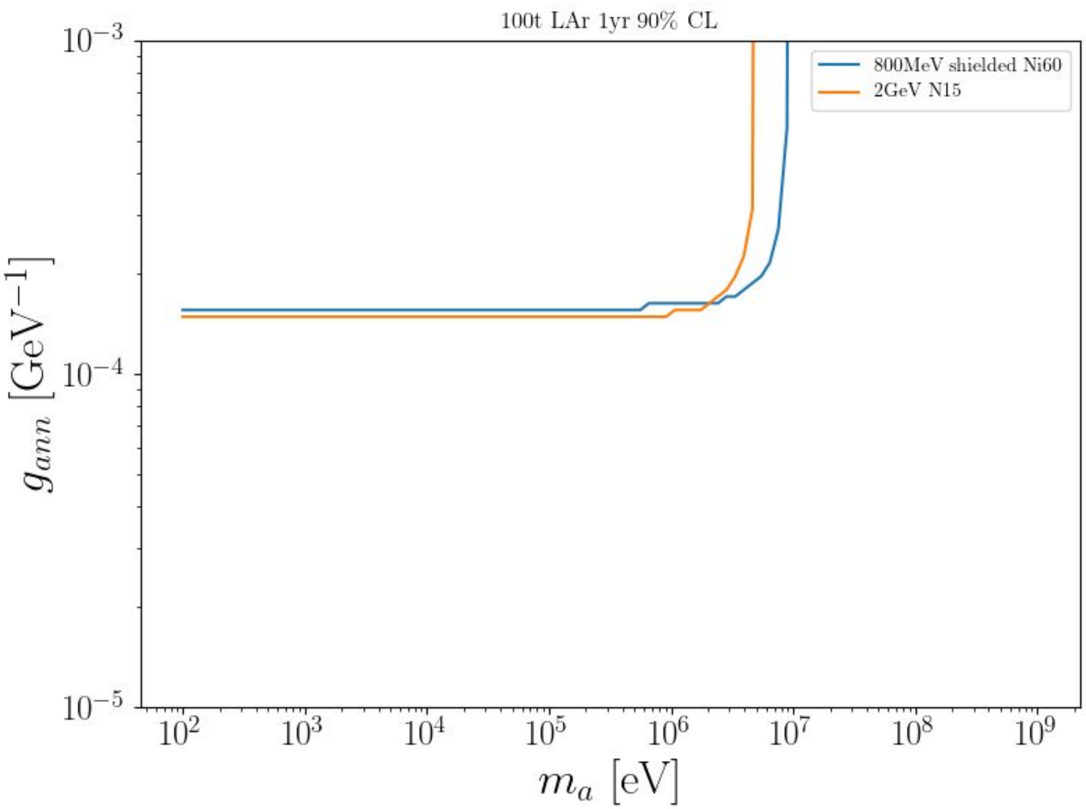

*axions don't decay

100t LAr, 1yr exposure
1e23 total POT

800MeV beam, shielded target: Ni60 9.38MeV
2GeV beam, C target: N15 5.266MeV

Source: primakoff
Detection: inv. primakoff, decay, absorption

MINER

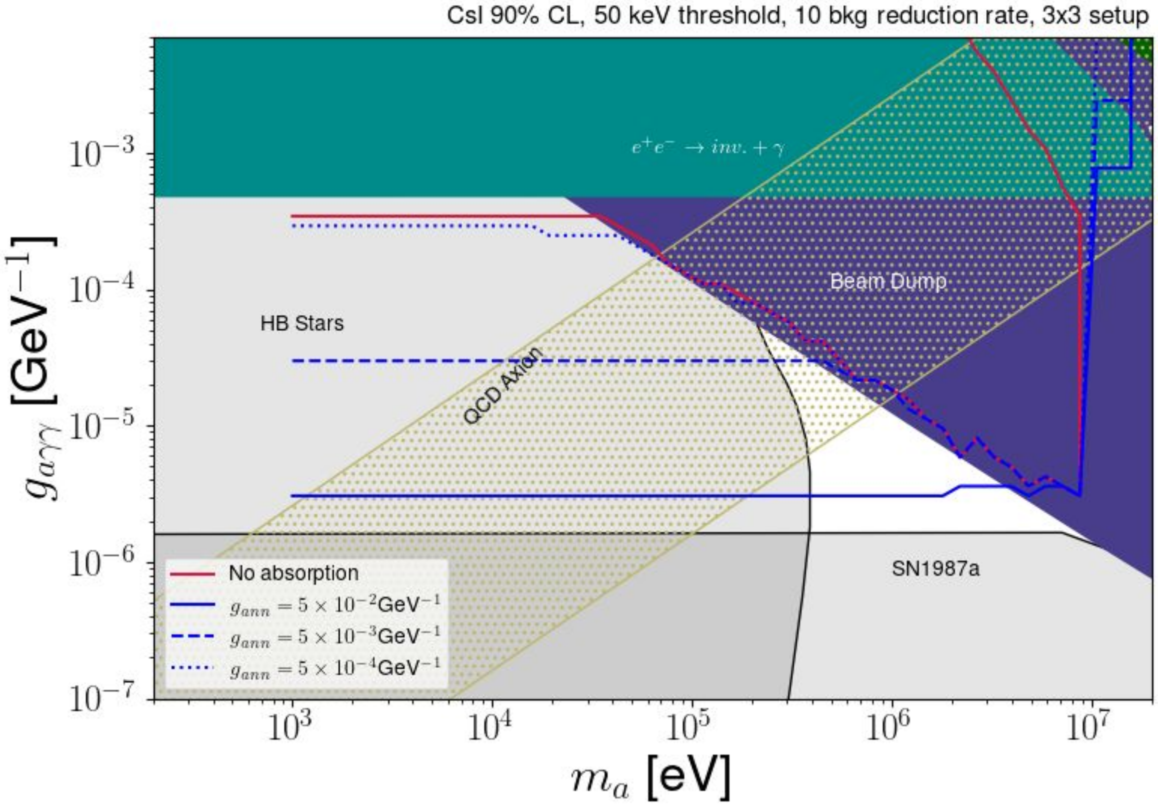

WIMP existing constraints